

Heating of a semi-infinite Hooke chain

Sergei D. Liazhkov^{1,2}

¹Peter the Great Saint-Petersburg Polytechnic University, St. Petersburg, Russia

²Institute for Problems in Mechanical Engineering of the Russian Academy of Sciences, St. Petersburg, Russia.

February 20, 2025

Abstract

We consider unsteady ballistic heat transport in a semi-infinite Hooke chain with a free end and an arbitrary heat source. An analytical description of the evolution of the kinetic temperature is proposed in both discrete (exact) and continuum (approximate) formulations. The continualization of the discrete solution for kinetic temperature is performed through a large-time asymptotic estimate of the fundamental solution of the dynamical problem for the instantly perturbed conservative semi-infinite chain at the fronts of the incident and reflected thermal waves. By analyzing the continuum solution, we observe that any instantaneous heat supply (i.e., a heat pulse) results in the anti-localization of the reflected thermal wave. We demonstrate that sudden point heat supply leads to a transition to a non-equilibrium steady state, which, unexpectedly, may exist even in the non-dissipative case. The results of this paper are expected to provide insight into the continuum description of nanoscale heat transport.

1 Introduction

In this paper, we address the problem of ballistic heat transport in a one-dimensional discrete medium. This is the nanoscale heat transport regime, in which quasiparticles (phonons) do not interact. Experimental observations indicate features, which violate the Fourier law and are characteristic of the ballistic regime. Specifically, these observations reveal a direct proportionality of thermal conductivity with sample size¹ (see, e.g., [4, 5, 6, 7, 8]), independence of thermal resistance from sample size (see, e.g., [4]) and an oscillation-like decay of the sinusoidal temperature profile (see, e.g., [9, 10]). The development of a full-fledged theory that allows for the description of the aforementioned experiments and (micro-)nanoscale heat transport as a whole is relevant for (micro-)nanoelectronics [12, 11, 13, 14, 15, 16, 17], photovoltaics [18], nuclear engineering [19, 20, 21], and other applications discussed in [22].

We consider the problem of thermal transport in one-dimensional chains undergoing external heat supply and heat exchange with the environment. In most theoretical works, the latter is described in the non-equilibrium steady state. Probably the first such work is [23], in which the temperature profile in the chain with the heat reservoirs is shown to be essentially constant within the chain (except at its ends). Subsequently, an analogous problem statement has been considered in many works. In particular, the presence of disorder [24], anharmonicity

¹This is the limiting case of a power-law dependence of thermal conductivity on sample size, where the heat transport regime is called either anomalous [1] or quasi-ballistic [2, 3]. The other limiting case is the independence of thermal conductivity from sample size, corresponding to the diffusive regime.

[25, 26], particle collisions [27], spatial inhomogeneities [28, 29], and magnetic fields [30, 31] have been taken into account. Despite significant progress in stationary problems, investigating non-stationary problems is required for a full-fledged understanding of heat propagation.

In [32], unsteady ballistic heat transport in a one-dimensional monoatomic harmonic lattice (i.e., in the infinite Hooke chain ²) lying in a viscous environment was studied. An analytical solution for the kinetic temperature was obtained using an approach that was later generalized in [34]. Although the steady-state kinetic temperature in the infinite square lattice was the focus, the equation describing non-stationary heat propagation was obtained (see Eq. (4.8) in this paper). Since describing heat propagation with scattering of thermal waves from a spatial inhomogeneity is important, developing analytical methods for non-stationary heat propagation with boundaries is of interest.

In the present paper, we study heat propagation in a one-dimensional semi-infinite free end Hooke chain undergoing external energy supply. This study continues from [35], where heat transport in the chain was considered in the case of an instantaneous thermal pulse. In this paper, discrete (exact) and continuum (approximate) descriptions of heat transport via kinetic temperature are proposed. The continuum solution is shown to mismatch with the discrete one at and near the boundary and thus to be inapplicable. Developing a new approach for the continuum description of the discrete solution is an open problem. It might seem that this can be achieved through kinetic theory. However, there are the following difficulties. On the one hand, solving the uncollisionless Boltzmann transport equation (BTE) with the evenness condition at the free end leads to the continuum solution described above (see Remark 1 in [35]), and therefore, this approach is unsuitable. On the other hand, the analysis of BTE with a collision term is also problematic. To the best of our knowledge, neither an effective approach to solve the equation with a collision term, corresponding to boundary scattering, nor the corresponding relaxation time is known. Therefore, we choose a route for continuum representation among those proposed in Sect. 7 of [35], namely, through asymptotic estimate of the discrete fundamental solution for the semi-infinite chain at the fronts of incident and reflected waves, as done in [36, 37] (see Sect. 5.2).

The paper is organized as follows. In Sect. 2, we discuss the notation. In Sect. 3, we formulate the stochastic dynamical problem, following the approach in [32]. In Sect. 4, we obtain an exact solution for the kinetic temperature. In Sect. 5, we present two ways to represent the discrete solution in the continuum limit: one through the principle of symmetry formulated in [35] (Sect. 5.1) and the other through the aforementioned approach described in Sect. 5.2. The purposes of this representation are, firstly, to simplify the obtained solution; secondly, to facilitate its interpretation from a physical point of view; and thirdly, to draw a parallel between (micro-)nanoscopic and macroscopic descriptions of heat transport. The obtained continuum solution for kinetic temperature is expected to be used as a constitutive relation in problems of ballistic thermoelasticity [38, 39] or thermoelectromagnetism (see, e.g., [40])³. In Sect. 5.3, we analyze the continuum solutions for kinetic temperature for the special case of instantaneous heat supply, i.e., the heat pulse. Using the new continuum solution, we show that the reason for the jump in kinetic temperature at the boundary, detected in [35], is its rapid decay (as $1/t^3$, where t is time). A similar phenomenon of the rapid decay of the wave-field near a spatial inhomogeneity, introduced in [42] and called «anti-localization», was considered in both continuum [42] and discrete problems [37, 43, 44]. Note that the anti-localization of reflected thermal wave in the semi-infinite free end Hooke chain has already been considered

²The term «Hooke chain» was introduced in [33].

³Since ballistic heat transport corresponds to extended irreversible thermodynamics [41], kinetic temperature and heat flux are the independent quantities. In the present paper, we focus on obtaining and analyzing the kinetic temperature only. The issue concerning the heat flux is a separate study and remains beyond the scope of the present paper.

in [44], where the velocity of the free end, undergone an initial heat pulse, was shown to decay as⁴ $1/t^{3/2}$. In present paper, we focus on anti-localization due to a heat pulse at arbitrary point (Sect. 5.3.1) and at arbitrary initial thermal profiles (Sect. 5.3.2). In Sect. 5.4, sudden heat supply is considered. The continuum solutions for kinetic temperature are obtained in integral form. Using these, we obtain a far-field asymptotic solution for kinetic temperature for the case of supply at any point. In Sect. 6, we compare the obtained analytical calculations for kinetic temperature with corresponding numerical results for the instantaneous heat pulse (Sects. 6.1, 6.2) and heat supply for non-dissipative (Sect. 6.3.1) and dissipative (Sect. 6.3.2) cases. In analyzing the non-dissipative case of sudden heat supply with constant intensity, we reveal quite unexpected results concerning the evolution of kinetic temperature within the chain (Sect. 6.3.1). Specifically, we show that kinetic temperature at the boundary tends to a stationary value, if the source is outside it. If the source is at the boundary, the kinetic temperature gradually tends to a stationary value along the chain. In Sect. 7, we provide a discussion of the results and ways to improve and generalize them.

2 Nomenclature

\mathbb{N} is the set of all natural numbers;

t is the time;

n is a particle number;

(\dots) and (\dots) stand for the first and second time derivatives respectively;

$H(\dots)$ is the Heaviside function;

$\delta_{n,j}$ is the Kronecker delta (1 if $n = j$ and 0 otherwise);

$\delta(t)$ is the Dirac delta function;

θ is the wave number;

ω_e is the elementary atomic frequency;

x is a continuum spatial coordinate;

a is the undeformed bond length;

J is the Bessel function of the first kind;

K is the modified Bessel function of the second kind.

3 Statement of the problem

We consider the semi-infinite Hooke chain, which has one free end. We assume that the chain is surrounded by a weakly viscous environment and that the motion of particles is triggered by the uncorrelated white noise. Therefore, the dynamics of particle n is governed by the following system of Langevin equations:

$$\begin{aligned} du_n &= v_n dt, \\ dv_n &= (\omega_e^2(u_{n+1} - u_n) - \omega_e^2(u_n - u_{n-1})(1 - \delta_{n,0}) - 2\eta v_n) dt + b_n dW_n, \quad n \in \mathbb{N} \cup \{0\}, \\ \omega_e &\stackrel{\text{def}}{=} \sqrt{c/m}, \quad dW_n = \rho_n \sqrt{dt}, \quad \langle \rho_n \rangle = 0, \quad \langle \rho_n \rho_{n'} \rangle = \delta_{n,n'}, \quad \eta \ll \omega_e, \end{aligned} \quad (1)$$

where u_n and v_n are displacement and velocity for n -th particle respectively; c is the bond stiffness; m is the mass of particle; ω_e is the elementary atomic frequency; η is a kinematic

⁴Earlier, this result was obtained in [45] and explained as «a consequence of the fact that the harmonic lattice does not forget its boundary condition, even in the thermodynamic limit». In that paper, the term «anti-localization» was not mentioned.

viscosity of the environment; W_n are uncorrelated Wiener processes; $\rho_n(t)$ are independent random variables with zero mean and unit variance; $\langle \dots \rangle$ stands for the expected value sign; $b_n(t)$ is an intensity of the stochastic excitation; $\delta_{n,j}$ is the Kronecker delta.

Remark 1. The form of Eqs. (1), which is given also in [32, 34] aside from the current work, is not only one form of the Langevin equations, and we use it because it seems more convenient to obtain the analytical solution. Another form (where the right part contains the term, corresponding to white noise, that is, \dot{W}) of these is shown in [46, 47].

Initially, all particles have zero displacement and velocities:

$$u_n(0) = 0, \quad v_n(0) = 0, \quad (2)$$

i.e., dynamics of the particles is induced by the stochastic excitation only.

4 An exact equation for the kinetic temperature

In this section, we derive an exact solution for the kinetic temperature. We consider an infinite set of realizations, which differ only by stochastic forces, related to uncorrelated Wiener processes. Due to simplicity of the considered model, we can characterize a thermal state via one parameter, which is referred to as a kinetic temperature:

$$k_B T_n \stackrel{\text{def}}{=} m \langle v_n^2 \rangle. \quad (3)$$

Remark 2. By the definition (3), we determine temperature as the kinetic temperature, that is, the average kinetic energy. Note that we use namely the definition «kinetic», because, firstly, the kinetic temperature is a quantity, which can be measured [48, 49, 50]. Secondly, it allows one to describe both non-stationary and stationary thermal states for one and the same system. On the other hand, there is the question of which average is suitable. In the present paper, the symbol $\langle \dots \rangle$ means the time average through which the kinetic temperature is defined, e.g., in [11, 51]. However, this quantity is often defined through the ensemble average (which is replaced by the average over realizations in numerical calculations [52, 53]), in particular, in regular papers of our scientific group (see, e.g., [66, 67, 68]). The latter definition is also correct in the thermodynamic limit due to, first, having been exactly derived [54] and, second, the deviation from ergodicity to tend to zero [59] (for the linear dynamical systems only)⁵. Note that an unambiguous definition of the temperature for systems far from equilibrium is still an unresolved fundamental problem [57, 60, 61].

Remark 3. We determine the kinetic temperature at one point, assuming that the distance between the unperturbed nearest particles (i.e., the undeformed bond length) to be the minimum size for the definition of temperature at the nanoscale. For detailed discussion on the size of the region over which the temperature can be defined, one can see in [11].

There are several approaches to obtain the kinetic temperature, obeying the definition (3). The covariance approach, namely, the introduction of all types of covariance of particle displacements and velocities and the derivation of deterministic equations with respect to these covariances, is considered in [32, 34] in the framework of the heat supply problem. The approach, based on the formulation of the Green function, is studied in [62]. An approach, which we use, is as follows.

To solve Eqs. (1), we use the direct and inverse discrete cosine transforms (DCT) [55]:

$$\hat{u}(\theta) = \sum_{n=0}^{\infty} u_n \cos \frac{(2n+1)\theta}{2}, \quad u_n = \frac{1}{\pi} \int_{-\pi}^{\pi} \hat{u}(\theta) \cos \frac{(2n+1)\theta}{2} d\theta, \quad (4)$$

where θ is the wave number; \hat{u} is some time-dependent function; $\hat{u}(\theta)$ is a some time-dependent function. The solution for particle velocity is sought in the same way because $\hat{v}(\theta) = \dot{\hat{u}}(\theta)$. The expression for v_n is further employed to obtain the kinetic temperature.

⁵The thoughts on ergodicity, related to general case, are discussed in [56, 57, 58].

Substitution of the formula (4) to the definition of the kinetic temperature (3) yields respectively:

$$\frac{k_B}{m} T_n = \frac{1}{\pi^2} \iint_{-\pi}^{\pi} \langle \hat{v}_1 \hat{v}_2 \rangle \cos \frac{(2n+1)\theta_1}{2} \cos \frac{(2n+1)\theta_2}{2} d\theta_1 d\theta_2, \quad [\dots]_i = [\dots](\theta_i), \quad (5)$$

where a is the length of undeformed bond between particles. Therefore, to obtain the kinetic temperature the covariance $\langle \hat{v}_1 \hat{v}_2 \rangle$ is yet to be obtained. Similarly, the problems of heat flux in the chain with reservoirs [63, 64] and energy growth in the Hooke chain [65] were solved. The next section is dedicated to solution with respect to the kinetic temperature in the semi-infinite chain.

4.1 The image of particle displacements and velocities

Applying (4) to the dynamic equations (1) with initial conditions (2) yields the following system with respect to \hat{u} and \hat{v} :

$$\begin{aligned} d\hat{u} &= \hat{v} dt, \\ d\hat{v} &= (-\omega^2 \hat{u} - 2\eta \hat{v}) dt + \sum_{n=0}^{\infty} b_n dW_n \cos \frac{(2n+1)\theta}{2}, \end{aligned} \quad (6)$$

where $\omega(\theta) \stackrel{\text{def}}{=} 2\omega_e \left| \sin \frac{\theta}{2} \right|$ is the dispersion relation for the Hooke chain, with initial conditions

$$\hat{u} = \hat{v} = 0, \quad (7)$$

We introduce a vector $\hat{\mathbf{u}}(\theta)$ such that

$$\hat{\mathbf{u}}(\theta) = \begin{pmatrix} \hat{u}(\theta) \\ \hat{v}(\theta) \end{pmatrix}. \quad (8)$$

The equations (6) are rewritten into the first-order stochastic differential equation in the matrix form:

$$d\hat{\mathbf{u}} = \mathbf{A} \hat{\mathbf{u}} dt + \mathbf{B} d\mathbf{W}, \quad (9)$$

$$\mathbf{A}(\theta) = \begin{pmatrix} 0 & 1 \\ -\omega^2(\theta) & -2\eta \end{pmatrix}, \quad \mathbf{B}(\theta) = \begin{pmatrix} 0 & 0 & \dots \\ b_0 \cos \frac{\theta}{2} & b_1 \cos \frac{3\theta}{2} & \dots \end{pmatrix}, \quad (10)$$

$$d\mathbf{W} = \begin{pmatrix} dW_0 \\ dW_1 \\ \dots \end{pmatrix}, \quad (11)$$

with initial condition

$$\hat{\mathbf{u}} = \mathbf{0}. \quad (12)$$

The following solution for $\hat{\mathbf{u}}$ is obtained in the form of the Itô integral (see Appendix A):

$$\hat{\mathbf{u}} = \int_0^t e^{\mathbf{A}(t-\tau)} \mathbf{B}(\tau) d\mathbf{W}. \quad (13)$$

Further, we employ the obtained solution for $\hat{\mathbf{u}}$ to find a variance matrix.

4.2 The variance matrix

We introduce the matrix \mathbf{D} such that

$$\mathbf{D} \stackrel{\text{def}}{=} \left\langle \left(\hat{\mathbf{u}}_1 - \langle \hat{\mathbf{u}}_1 \rangle \right) \otimes \left(\hat{\mathbf{u}}_2 - \langle \hat{\mathbf{u}}_2 \rangle \right) \right\rangle, \quad (14)$$

where \otimes stands for the dyadic product of vectors⁶. Due to the initial condition (12), the mathematical expectation of $\hat{\mathbf{u}}$ equals zero. We rewrite \mathbf{D} in the form

$$\mathbf{D} = \left\langle \hat{\mathbf{u}}_1 \otimes \hat{\mathbf{u}}_2 \right\rangle = \begin{pmatrix} \langle \hat{u}_1 \hat{u}_2 \rangle & \langle \hat{u}_1 \hat{v}_2 \rangle \\ \langle \hat{v}_1 \hat{u}_2 \rangle & \langle \hat{v}_1 \hat{v}_2 \rangle \end{pmatrix}. \quad (15)$$

Therefore, the variance matrix \mathbf{D} is a covariance matrix, elements of which are covariances of images of velocities and displacements. On the other hand, \mathbf{D} can be calculated by substitution of the $\hat{\mathbf{u}}$ (13) to (15) and simplification using uncorrelatedness of the Wiener processes. This yields (see Appendix B)

$$\mathbf{D} = \int_0^t e^{\mathbf{A}_1(t-\tau)} (\mathbf{B}_1(\tau) \mathbf{B}_2^\top(\tau)) e^{\mathbf{A}_2^\top(t-\tau)} d\tau, \quad (16)$$

where $\mathbf{A}_i = \mathbf{A}(\theta_i)$; $\mathbf{B}_i = \mathbf{B}(\theta_i)$; \top stands for the transpose sign. The sought covariance $\langle \hat{v}_1 \hat{v}_2 \rangle$ is then found as D_{22} . If necessary, the elements D_{12} and D_{21} may be used to obtain the heat flux⁷.

4.3 The discrete solution for the kinetic temperature in the semi-infinite chain

Having multiplied matrices, containing in the integrand of \mathbf{D} subsequently and having taken D_{22} , we obtain

$$\begin{aligned} \langle \hat{v}_1 \hat{v}_2 \rangle &= \sum_{n=0}^{\infty} b_n^2(t) * \left(e^{-2\eta t} \prod_{i=1,2} \cos \frac{(2n+1)\theta_i}{2} \varphi_i(t) \right), \\ \varphi_i(t) &= \cos \left(t \sqrt{\omega(\theta_i)^2 - \eta^2} \right) - \frac{\eta \sin \left(t \sqrt{\omega(\theta_i)^2 - \eta^2} \right)}{\sqrt{\omega(\theta_i)^2 - \eta^2}}, \end{aligned} \quad (17)$$

$$X(t) * Y(t) \stackrel{\text{def}}{=} \int_0^t X(\tau) Y(t-\tau) d\tau = \int_0^t X(t-\tau) Y(\tau) d\tau.$$

Following [32], introduce a function of heat supply intensity such that

$$k_B \chi_n \stackrel{\text{def}}{=} \frac{m}{2} b_n^2, \quad \chi_n|_{t < 0} = 0. \quad (18)$$

Substitution of (17) to (5), taking into account (18) and property of multiplication of the

⁶ $\{\mathbf{X} \otimes \mathbf{Y}\}_{ij} = X_i Y_j$.

⁷The expression for the heat flux contains covariances of the displacements and velocities (see, e.g., [70]).

integrals yields the following equation for the kinetic temperature:

$$T_n = 2 \sum_{j=0}^{\infty} \chi_j(t) * (e^{-2\eta t} \mathbb{I}_{n,j}^2(t)),$$

$$\mathbb{I}_{n,j}(t) \stackrel{\text{def}}{=} \frac{1}{\pi} \int_{-\pi}^{\pi} \cos \frac{(2j+1)\theta}{2} \cos \frac{(2n+1)\theta}{2} \left(\cos \left(t \sqrt{\omega(\theta)^2 - \eta^2} \right) - \frac{\eta \sin \left(t \sqrt{\omega(\theta)^2 - \eta^2} \right)}{\sqrt{\omega(\theta)^2 - \eta^2}} \right) d\theta. \quad (19)$$

For $\eta \ll \omega_e$, we simplify the latter, that is

$$T_n = 2 \sum_{j=0}^{\infty} \chi_j(t) * \left(e^{-2\eta t} \dot{\Phi}_{n,j}^2(t) \right) + O\left(\frac{\eta}{\omega_e}\right), \quad (20)$$

$$\dot{\Phi}_{n,j}(t) \stackrel{\text{def}}{=} \frac{1}{\pi} \int_{-\pi}^{\pi} \cos \frac{(2j+1)\theta}{2} \cos \frac{(2n+1)\theta}{2} \cos(\omega(\theta)t) d\theta,$$

where we use $\sqrt{\omega^2 - \eta^2} \approx \omega$. Further, we drop out the terms up to order of $O(\eta/\omega_e)$ and further refer (20) to as the *discrete solution* for the kinetic temperature. Note that the second expression in (20) satisfies the following problem [35]:

$$\ddot{\Phi}_n = \omega_e^2 (\Phi_{n+1} - \Phi_n) - \omega_e^2 (\Phi_n - \Phi_{n-1})(1 - \delta_{n,0}) + \delta_{n,j} \delta(t). \quad (21)$$

where $\delta(\dots)$ is the Dirac delta function and δ_{\dots} is the Kronecker delta, corresponding to the dynamics of the semi-infinite chain after instantaneous perturbation of the particle j by the unit magnitude. The equation (21) is supplemented by the initial condition for Φ_n , written in the generalized form [71]:

$$\Phi_n|_{t<0} = 0. \quad (22)$$

Based on aforesaid and on the linearity of the problem, we write the structure of the discrete solution for the kinetic temperature in the Hooke chain with *arbitrary* boundary conditions:

$$T_n = 2 \sum_{j \in \mathbb{P}} \chi_j(t) * \left(e^{-2\eta t} \dot{\Phi}_{n,j}^2(t) \right), \quad \ddot{\Phi}_n = \omega_e^2 \mathcal{L}_n \Phi_n - 2\eta \dot{\Phi}_n + \delta_{n,j} \delta(t), \quad (23)$$

where \mathcal{L}_n is the linear difference operator, which depends on specific boundary conditions; \mathbb{P} is set of numbers, by which the perturbed particles in the system are indexed. Note that Eq. (23) is valid for $\eta \ll \omega_e$ only⁸.

5 Kinetic temperature in the continuum limit

In the case of arbitrary heat source, χ , the formula (20) becomes hard to use. Therefore (and for other reasons, described in Sect. 1), we derive the kinetic temperature in a continuum limit, i.e., as a continuum coordinate function, x . We present approaches to attain the latter in the following.

5.1 The first approach

The first approach is based on using the continuum solution for the kinetic temperature, in the *infinite* chain, obtained in [32]:

$$T(t, x) = \int \int_{-\infty}^{\infty} \chi(\tau, \xi) \mathcal{G}(t - \tau, x - \xi) d\xi d\tau, \quad (24)$$

⁸For arbitrary η , the function $\dot{\Phi}_{n,j}^2$ in Eq. (23) must be replaced by $(\dot{\Phi}_{n,j} - \eta \Phi_{n,j})^2$ and $\omega(\theta)$ by $\sqrt{\omega(\theta)^2 - \eta^2}$.

$$\mathcal{G}(t, x) \stackrel{\text{def}}{=} \frac{H(v_s t - |x|)e^{-2\eta t}}{\pi \sqrt{v_s^2 t^2 - x^2}}, \quad (25)$$

where $v_s \stackrel{\text{def}}{=} \omega_e a$ is the speed of sound; H is the Heaviside function; $\mathcal{G}(t, x)$ is the fundamental solution for the problem of heat transport in the infinite Hooke chain, lying in a viscous environment [32]; $T(t, x)$ and $\chi(t, x)$ are respectively the continuum functions of the kinetic temperature and the heat supply intensity, such as

$$T(an, t) \equiv T_n(t), \quad \chi(an, t) \equiv \chi_n(t). \quad (26)$$

Applying the principle of symmetry of the continuum solution [35], we rewrite the equation for the kinetic temperature in the semi-infinite chain:

$$\begin{aligned} T(t, x) &= \iint_{-\infty}^{\infty} \chi(\tau, |\xi|) \mathcal{G}(t - \tau, x - \xi) d\xi d\tau = \frac{1}{\pi} \int_0^{\infty} \int_{\frac{|x-\xi|}{v_s}}^t \chi(\tau, \xi) \frac{e^{-2\eta(t-\tau)} d\tau d\xi}{\sqrt{v_s^2(t-\tau)^2 - (x-\xi)^2}} \\ &+ \frac{1}{\pi} \int_0^{\infty} \int_{\frac{x+\xi}{v_s}}^t \chi(\tau, \xi) \frac{e^{-2\eta(t-\tau)} d\tau d\xi}{\sqrt{v_s^2(t-\tau)^2 - (x+\xi)^2}}. \end{aligned} \quad (27)$$

The last identity is rewritten due to the function χ is finite. Thus, a continuum solution for the semi-infinite chain can be obtained in the case of an arbitrary heat supply source. We refer the latter to as a *symmetrical continuum solution*⁹.

5.2 The second approach

The second approach is based on the direct continualization procedure of the discrete solution (20). The continualization can be performed in two ways. The first, namely, the averaging of the discrete solution over a mesoscale, the order of which is more than a but less than the chain length, is described in detail in [35, 69]. Applying it to the current problem obviously yields the symmetrical continuum solution, because the principle of symmetry of the continuum solution, formulated in [35], is the corollary of the method of continualization described above. The second way is presented below.

In [35] the problem (Eqs. (21), (22)) was shown to be equivalent to the problem for the infinite chain with the same source in the particle j and the mirrored source with respect to the center symmetry. In the framework of the discrete problem, it is *not* 0-th particle but rather *the bond* between the 0-th and -1 -th particles. Therefore, the problem, governed by Eq. (21) is equivalent to the following one for the infinite chain:

$$\ddot{\Phi}_n = \omega_e^2 (\Phi_{n+1} - 2\Phi_n + \Phi_{n-1}) + (\delta_{n,j} + \delta_{n,-j-1}) \delta(t). \quad (28)$$

In turn, the equation (28) with the initial condition (22) is equivalent to the following initial-valued problem:

$$\ddot{\Phi}_n = \omega_e^2 (\Phi_{n+1} - 2\Phi_n + \Phi_{n-1}), \quad (29)$$

$$\Phi_n = 0, \quad \dot{\Phi}_n = \delta_{n,j} + \delta_{n,-j-1}, \quad (30)$$

solution of which is written as follows¹⁰:

$$\dot{\Phi}_{n,j} = J_{2|n-j|}(2\omega_e t) + J_{2|n+j+1|}(2\omega_e t), \quad (31)$$

⁹In the non-dissipative case ($\eta \rightarrow 0+$), the function \mathcal{G} , defined by Eq. (25) is the well-known fundamental solution of the problem of ballistic heat transport in the Hooke chain, which was derived in the frameworks in both the lattice dynamics approach [72, 67, 73, 69] and the kinetic theory [69].

¹⁰The Eq. (31) is written by using the fundamental solution for the infinite chain, according to [46, 74].

where J is the Bessel function of the first kind. For the semi-infinite chain, the Eq. (31) represents a superposition of the running wave, incident in the point j , and reflected from the boundary wave (described by the first and second terms, respectively). Furthermore, considering the semi-infinite chain, we omit the sign of the absolute value in the index of the second term in Eq. (31).

We perform a large-time asymptotic estimate of the function $\dot{\Phi}$ at the fronts of incident and reflected waves, using the technique proposed in [36]¹¹, based on the stationary phased approximation. That is, the first and second terms in (31) are estimated at the fronts of incident and reflected waves, respectively. Having done the latter, we write the estimate for $\dot{\Phi}_{n,j}$ as sum of the two harmonics, namely

$$\dot{\Phi}_{n,j} \sim \check{\Phi}_{|n-j|} H(\omega_e t - |n-j|) + \check{\Phi}_{n+j+1} H(\omega_e t - (n+j+1)), \quad (32)$$

$$\check{\Phi}_n \stackrel{\text{def}}{=} \sqrt{\frac{1}{\pi \sqrt{\omega_e^2 t^2 - n^2}}} \cos\left(\mathcal{W}_n t - \frac{\pi}{4}\right), \quad \mathcal{W}_n(t) \stackrel{\text{def}}{=} 2\omega_e \left(\sqrt{1 - \frac{n^2}{\omega_e^2 t^2}} - \frac{n}{\omega_e t} \arccos \frac{n}{\omega_e t} \right), \quad (33)$$

where \sim stands for the sign of the large-time asymptotically equivalent function; \mathcal{W}_n is referred to as a characteristic frequency of the natural oscillations in the Hooke chain such that the frequencies of the incident and reflected waves are $\mathcal{W}_{|n-j|}$ and \mathcal{W}_{n+j+1} respectively. Since the index, corresponding to the latter is more for all j and n , the frequencies of the incident and reflected waves are *not* equal, what is not in consistent to the continuum theory (see, e.g., [75]). Having analyzed the difference between the frequencies of the incident and reflected waves, $\Delta\mathcal{W} \stackrel{\text{def}}{=} \mathcal{W}_{|n-j|} - \mathcal{W}_{n+j+1}$, we suppose it to be negligible when $j=0$ and when $n=0$. In order to confirm the supposition, we put $j=0$ and expand $\Delta\mathcal{W}$ into series at $1/\omega_e t = 0$. The latter yields

$$\Delta\mathcal{W}|_{j=0} = \frac{\pi}{t} - \frac{2n+1}{\omega_e t^2} + O((\omega_e t)^{-3}). \quad (34)$$

The estimation for $\Delta\mathcal{W}|_{n=0}$ satisfies Eq. (34) with n replaced by j . Therefore, at large times $\Delta\mathcal{W} \ll \omega_e$ at $n=0 \forall j$ and at $j=0 \forall n$. This observation is important for asymptotic analysis of the expression for the thermal fundamental solution, $\dot{\Phi}_{nj}^2$.

In order to analyze the expression for the kinetic temperature (Eq. (20)) write separately asymptotic estimate for the $\dot{\Phi}_{n,j}^2$:

$$\begin{aligned} \dot{\Phi}_{nj}^2 \sim \check{\Phi}_{nj}^2 \stackrel{\text{def}}{=} & \frac{1 + \sin(2\mathcal{W}_{|n-j|}t)}{2\pi \sqrt{\omega_e^2 t^2 - (n-j)^2}} H(\omega_e t - |n-j|) + \frac{1 + \sin(2\mathcal{W}_{n+j+1}t)}{2\pi \sqrt{\omega_e^2 t^2 - (n+j+1)^2}} H(\omega_e t - (n+j+1)) \\ & + \frac{\sin((\mathcal{W}_{|n-j|} + \mathcal{W}_{n+j+1})t) + \cos((\mathcal{W}_{|n-j|} - \mathcal{W}_{n+j+1})t)}{\pi^4 \sqrt{(\omega_e^2 t^2 - (n-j)^2)(\omega_e^2 t^2 - (n+j+1)^2)}} H(\omega_e t - (n+j+1)). \end{aligned} \quad (35)$$

We refer the expression (35) to as a thermal fundamental solution. The first term in the latter is represented as a contribution of the running wave, and the second and third terms are contributions of the reflected wave. Following [36, 43], we separate the thermal fundamental solution previously as

$$\dot{\Phi}_{nj}^2 = \dot{\check{\Phi}}_{nj}^2 + \dot{\hat{\Phi}}_{nj}^2, \quad (36)$$

$$\dot{\check{\Phi}}_{nj}^2 \stackrel{\text{def}}{=} \frac{H(\omega_e t - |n-j|)}{2\pi \sqrt{\omega_e^2 t^2 - (n-j)^2}} + \frac{H(\omega_e t - (n+j+1))}{2\pi \sqrt{\omega_e^2 t^2 - (n+j+1)^2}}, \quad (37)$$

¹¹For the first time (for discrete media), this approach was used in [36] to estimate the fundamental solution for the infinite Hooke chain.

$$\begin{aligned} \dot{\Phi}_{nj}^2 \stackrel{\text{def}}{=} & \frac{H(\omega_e t - |n-j|) \sin(2\mathcal{W}_{|n-j|} t)}{2\pi\sqrt{\omega_e^2 t^2 - (n-j)^2}} + \frac{H(\omega_e t - (n+j+1)) \sin(2\mathcal{W}_{n+j+1} t)}{2\pi\sqrt{\omega_e^2 t^2 - (n+j+1)^2}} \\ & + \frac{H(\omega_e t - (n+j+1)) \sin((\mathcal{W}_{|n-j|} + \mathcal{W}_{n+j+1}) t)}{\pi^4\sqrt{(\omega_e^2 t^2 - (n-j)^2)(\omega_e^2 t^2 - (n+j+1)^2)}} + \frac{H(\omega_e t - (n+j+1)) \cos((\mathcal{W}_{|n-j|} - \mathcal{W}_{n+j+1}) t)}{\pi^4\sqrt{(\omega_e^2 t^2 - (n-j)^2)(\omega_e^2 t^2 - (n+j+1)^2)}}, \end{aligned} \quad (38)$$

where $\dot{\Phi}_{nj}^2$ and $\dot{\Phi}_{nj}^2$ are the slow and conditionally fast motions components respectively. The conditionally fast motion component represents the sum of four harmonics. However, since the first two harmonics correspond to the transient process, related with equilibration of the kinetic and potential energies, we neglect these. Since the characteristic frequencies of incident and reflected waves are close to each others when $j = 0 \forall n$ and for $n = 0 \forall j$ (see Eq. (34)), the last harmonic in Eq. (38) transforms to a slow quantity. We conclude that the perturbation at the boundary *dramatically* changes the character of thermal wave propagation. A possible physical explanation of the latter may lie in the effect of interference of incident and reflected thermal waves, which occurs instantly after the beginning of the perturbation and is described by the third in fourth terms of $\dot{\Phi}_{nj}^2$ (see Eq. (38)). The farther the source from the boundary, the weaker the interference of the reflected and incident waves, because their energy is lost due to dispersion and (a fortiori) viscosity.

Techniques of continualization of the solution for the kinetic temperature (20) are presented below for the different types of heat source.

5.3 Case of instantaneous heat perturbation

We consider the special case of heat supply, namely, an instantaneous heat perturbation (i.e., heat pulse) and the absence of dissipation. The heat supply intensity, χ , is defined as

$$\chi_n(t) = \frac{1}{2} T_n^0 \delta(t), \quad (39)$$

where T_n^0 is the initial kinetic temperature profile.

Remark 4. Initial heat pulse, which is mathematically expressed in (39) by the Dirac delta function, physically corresponds to the supply, having performed for the *finite* time, which is much less in comparison with the time of atom excitation. This type of supply is regularly realized in the experiments, e.g., with femtosecond (see, e.g., [77]) and attosecond (see [78] and references there) lasers.

By using the first expression in (20) with taking into account (31), tending $\eta \rightarrow 0+$ in it, we write the discrete solution for the kinetic temperature as

$$T_n = \sum_{j=0}^{\infty} T_j^0 \dot{\Phi}_{n,j}^2 = \sum_{j=0}^{\infty} T_j^0 (J_{2|n-j|}(2\omega_e t) + J_{2(n+j+1)}(2\omega_e t))^2. \quad (40)$$

The form of the discrete solution for the kinetic temperature (40)¹² is much simpler than the one obtained in [35] (see Eq. (11) therein). Note that the *same* equation for the discrete solution may be obtained through the random velocity initial problem (with the corresponding initial kinetic temperature profile), where the kinetic temperature is determined as the ensemble (not time, as we initially introduce in Eq. (3)) average.

Further, we perform a continualization of this solution for the point and arbitrary heat sources.

¹²In Eq. (40) the factor $H(t)$ can be omitted due to the condition for χ_n (see (18)) is fulfilled in the expression (20).

5.3.1 Point heat pulse. The anti-localization of reflected thermal wave

Consider the point heat perturbation, defined as

$$T_n^0 = T^0 \delta_{n,j}, \quad k_B T^0 \stackrel{\text{def}}{=} m v_s^2, \quad (41)$$

where T^0 is the amplitude of initial kinetic temperature; j is the number of the point, undergone the pulse. In this case, the discrete solution for the kinetic temperature equals to the thermal fundamental solution, multiplied by T^0 :

$$T_n = T^0 \left(J_{2|n-j|}(2\omega_e t) + J_{2(n+j+1)}(2\omega_e t) \right)^2. \quad (42)$$

We introduce the function $g(t, x, \xi)$ such as

$$ag(t, na, ja) \stackrel{\text{def}}{=} \dot{\Phi}_{n,j}^2. \quad (43)$$

Therefore, the function g may also be separated correspondingly to the slow and conditionally fast motions as

$$g(t, x, \xi) = \bar{g}(t, x, \xi) + \hat{g}(t, x, \xi), \quad (44)$$

where \bar{g} is function, which is further referred as to a kernel of the fundamental solution has the form

$$\bar{g}(t, x, \xi) = \left[\begin{array}{l} \frac{H(v_s t - |x - \xi|)}{2\pi \sqrt{v_s^2 t^2 - (x - \xi)^2}} + \frac{H(v_s t - (x + \xi + a))}{2\pi \sqrt{v_s^2 t^2 - (x + \xi + a)^2}}, \quad \forall x, \xi > 0, \\ \\ \frac{H(v_s t - x)}{2\pi \sqrt{v_s^2 t^2 - x^2}} \\ + \frac{H(v_s t - (x + a))}{2\pi \sqrt{v_s^2 t^2 - (x + a)^2}} + \frac{\cos((\mathcal{W}(x) - \mathcal{W}(x + a))t) H(v_s t - (x + a))}{\pi^4 \sqrt{(v_s^2 t^2 - x^2)(v_s^2 t^2 - (x + a)^2)}}, \quad \xi = 0 \quad \forall x, \\ \\ \frac{H(v_s t - \xi)}{2\pi \sqrt{v_s^2 t^2 - \xi^2}} \\ + \frac{H(v_s t - (\xi + a))}{2\pi \sqrt{v_s^2 t^2 - (\xi + a)^2}} + \frac{\cos((\mathcal{W}(\xi) - \mathcal{W}(\xi + a))t) H(v_s t - (\xi + a))}{\pi^4 \sqrt{(v_s^2 t^2 - \xi^2)(v_s^2 t^2 - (\xi + a)^2)}}, \quad x = 0 \quad \forall \xi, \end{array} \right. \quad (45)$$

where $\mathcal{W}(x)$ is a continuous function of the characteristic frequency such as

$$\mathcal{W}(na, t) \equiv \mathcal{W}_n(t). \quad (46)$$

Neglecting the fast motions and simplifying (45), we write the continuum solution for the kinetic temperature as

$$T(t, x) \approx \mathcal{A} \left[\begin{array}{l} \frac{H(v_s t - |x - \xi|)}{2\pi\sqrt{v_s^2 t^2 - (x - \xi)^2}} + \frac{H(v_s t - (x + \xi + a))}{2\pi\sqrt{v_s^2 t^2 - (x + \xi + a)^2}}, \quad \forall x, \xi > 0, \\ \\ \frac{H(v_s t - x)}{2\pi\sqrt{v_s^2 t^2 - x^2}} \\ + \frac{H(v_s t - (x + a))}{2\pi\sqrt{v_s^2 t^2 - (x + a)^2}} + \frac{\left(-1 + \frac{(a+2x)^2}{2v_s^2 t^2}\right) H(v_s t - (x + a))}{\pi^4 \sqrt{(v_s^2 t^2 - x^2)(v_s^2 t^2 - (x + a)^2)}}, \quad \xi = 0 \quad \forall x, \\ \\ \frac{H(v_s t - \xi)}{2\pi\sqrt{v_s^2 t^2 - \xi^2}} \\ + \frac{H(v_s t - (\xi + a))}{2\pi\sqrt{v_s^2 t^2 - (\xi + a)^2}} + \frac{\left(-1 + \frac{(a+2\xi)^2}{2v_s^2 t^2}\right) H(v_s t - (\xi + a))}{\pi^4 \sqrt{(v_s^2 t^2 - \xi^2)(v_s^2 t^2 - (\xi + a)^2)}}, \quad x = 0 \quad \forall \xi, \end{array} \right] \quad (47)$$

where $\mathcal{A} \stackrel{\text{def}}{=} T^0 a$ is a constant of $\text{K} \cdot \text{m}$ dimension. Consider the kinetic temperature at the boundary. Expanding the expression (47) for $x = 0$ into series at $\omega_e t = \infty$ yields

$$T(t, 0) \sim \frac{\mathcal{A}(a + 2\xi)^2}{2\pi v_s^3 t^3}, \quad (48)$$

i.e., the continuum solution at the boundary decays as $1/t^3$. For comparison, we recall that the symmetrical continuum solution has the form [35]

$$T(t, x) = \frac{\mathcal{A}}{2\pi} \left(\frac{H(v_s t - |x - \xi|)}{\sqrt{v_s^2 t^2 - (x - \xi)^2}} + \frac{H(v_s t - |x + \xi|)}{\sqrt{v_s^2 t^2 - (x + \xi)^2}} \right), \quad (49)$$

which can also be obtained by substitution of the continuum heat source function, defined as

$$\chi(t, x) = \frac{T^0}{2} \delta(x - \xi) \delta(t), \quad (50)$$

to the expression (27) for $\eta \rightarrow 0+$. Note that the symmetrical continuum solution at the boundary decays as $1/t$, what is significantly slower than the continuum solution. From (48), we conclude the anti-localization of the reflected thermal wave to be observed. Moreover, this phenomenon occurs after perturbation at any point. We suppose that the anti-localization is associated with interaction between the incident and reflected waves, because the crucial contribution to the kinetic temperature comes from the term ΔT_B .

Based on investigations done above and simplifications of (47), we construct the final continuum solution for the case of point heat pulse:

$$T(t, x) \approx \mathcal{A} \left[\begin{array}{l} \frac{H(v_s t - |x - \xi|)}{2\pi\sqrt{v_s^2 t^2 - (x - \xi)^2}} + \left(\frac{1}{2\pi\sqrt{v_s^2 t^2 - (x + \xi + a)^2}} + \delta f(\xi, t) \right) H(v_s t - (x + \xi + a)), \quad \xi > 0, \quad x = 0, \\ \\ \frac{H(v_s t - |x - \xi|)}{2\pi\sqrt{v_s^2 t^2 - (x - \xi)^2}} + \frac{H(v_s t - (x + \xi + a))}{2\pi\sqrt{v_s^2 t^2 - (x + \xi + a)^2}}, \quad \xi > 0, \quad x > 0, \\ \\ \frac{H(v_s t - x)}{2\pi\sqrt{v_s^2 t^2 - x^2}} + \left(\frac{1}{2\pi\sqrt{v_s^2 t^2 - (x + a)^2}} + \delta f(t, x) \right) H(v_s t - (x + a)), \quad \xi = 0, \end{array} \right] \quad (51)$$

$$\delta f(t, x) \stackrel{\text{def}}{=} -\frac{1}{\pi v_s t} + \frac{(a^2 + 6ax + 6x^2)}{4\pi v_s^3 t^3} + O((\omega_\epsilon t)^{-5}). \quad (52)$$

Note that the continuum solution is invalid on the leading fronts of the incident and reflected thermal waves. The asymptotic solution for the kinetic temperature in this case should be calculated in another way. Since the reflection of thermal wave does not influence the propagation of the incident one, the asymptotic solution for the kinetic temperature on the leading front of latter is expected to be the same as one for the infinite Hooke chain [80]. Asymptotic analysis of the kinetic temperature on the leading front of the reflected wave is beyond the scope of present paper.

5.3.2 Arbitrary heat pulse

Introduce the continuum function of initial kinetic temperature such that

$$T^0(an) \equiv T_n^0. \quad (53)$$

Then the continuum solution can be constructed by rewriting of Eq. (40) with replacement of T_n by $T(t, x)$, $\dot{\Phi}_{n,j}^2$ by $ag(t, x, \xi)$ and \sum_j by $\frac{1}{a} \int_0^\infty \dots d\xi$. Taking into account both the fast and slow processes, we obtain the following expression for the kinetic temperature:

$$T(t, x) = \frac{1}{2\pi} \int_0^\infty \frac{T^0(\xi) H(v_s t - |x - \xi|) d\xi}{\sqrt{v_s^2 t^2 - (x - \xi)^2}} + \frac{1}{2\pi} \int_0^\infty \frac{T^0(\xi) H(v_s t - (x + \xi + a)) d\xi}{\sqrt{v_s^2 t^2 - (x + \xi + a)^2}} + \Delta T_B, \quad (54)$$

$$\Delta T_B(t, x) \stackrel{\text{def}}{=} \frac{1}{\pi} \int_0^\infty T^0(\xi) H(v_s t - (x + \xi + a)) \Delta g(t, x, \xi)|_{q=1} d\xi, \quad (55)$$

$$\Delta g(t, x, \xi) \stackrel{\text{def}}{=} \frac{q \sin((\mathcal{W}(|x - \xi|) + \mathcal{W}(x + \xi + a))t) + \cos((\mathcal{W}(|x - \xi|) - \mathcal{W}(x + \xi + a))t)}{\sqrt[4]{(v_s^2 t^2 - (x - \xi)^2)(v_s^2 t^2 - (x + \xi + a)^2)}}. \quad (56)$$

Here ΔT_B is a term, corresponding influence of the free boundary of thermal processes; q is a constant, which is equal to 1 if the fast oscillation term is included in the expression for the ΔT_B and 0 otherwise.

Note that the expression for the kinetic temperature (54) contains the term, corresponding to the oscillating term \hat{g} . Taking into account this term may result in oscillations of the kinetic temperature as functions near the points of particle location. Therefore, the solution for the kinetic temperature itself is not classified as a continuum but rather as a *discrete-continuum* solution. From the expression (48) and Eq. (54) it follows that *any* initial instantaneous thermal perturbation results in the anti-localization of the reflected thermal wave.

Remark 5. From the expression (48) it follows that the anti-localization of thermal waves is enhanced, as the source approaches the boundary. This case is equivalent to fast decay of the kinetic temperature field in the infinite chain between two heat mirrored sources, which are close to each other and their sizes are less than the distance between them. This effect, caused by thermal wave interference, was experimentally observed in [79]. In this work, the authors refer the heat transfer regime, at which the described above effect manifests, to as the collectively diffusive regime, which, as the authors argue, differs from the ballistic regime.

With accordance to the properties of the functions $\dot{\Phi}_{0j}^2$ and $\dot{\Phi}_{n0}^2$, described in Sect. 5.2, the *continuum* solution is constructed analogously as the discrete-continuum one by rewriting the

expression for ΔT_B (neglecting the fast-oscillating term in Δg) as follows:

$$\Delta T_B(t, x) = \begin{cases} \frac{1}{\pi} \int_0^\infty T^0(\xi) H(v_s t - (x + \xi + a)) \delta f(\xi, t) d\xi, & T^0(0) = 0, \\ \frac{1}{\pi} \int_0^\infty T^0(\xi) H(v_s t - (\xi + a)) \delta f(\xi, t) d\xi, & T^0(0) \neq 0, x = 0, \\ 0, & T^0(0) \neq 0, x \neq 0. \end{cases} \quad (57)$$

We recall that the symmetrical continuum solution has the form [35]

$$T(t, x) = \frac{T^0(x)}{2} J_0(4\omega_e t) + \frac{1}{2\pi} \int_0^\pi T^0(|x + v_s t \cos \theta|) d\theta, \quad (58)$$

where the first term corresponds to the process of equilibration of the kinetic and potential energies and the second term corresponds to the evolution of the kinetic temperature, caused by ballistic heat transport. At large times (after reflection of thermal wave) the first term may be negligible, and the symmetrical continuum solution has a simple form, which can also be obtained by substitution of the continuum heat source function, defined as

$$\chi(t, x) = \frac{T^0(x)}{2} \delta(t), \quad (59)$$

to the expression (27) at $\eta \rightarrow 0+$. Recall that the symmetrical continuum solution implies the source $T^0(x)$ to be continuous function at a distance of order at least two dozen particles [35]. This condition has no force for the continuum and discrete-continuum solutions.

5.4 General case. Example: sudden point heat supply

We construct the discrete-continuum solution in the same way as discussed in Sect. 5.3. Taking into account both the fast and slow processes, we obtain the following expression for the kinetic temperature:

$$T(t, x) = \frac{1}{\pi} \int_0^\infty \int_{\frac{|x-\xi|}{v_s}}^t \frac{\chi(\tau, \xi) e^{-2\eta(t-\tau)} d\tau d\xi}{\sqrt{v_s^2(t-\tau)^2 - (x-\xi)^2}} + \frac{1}{\pi} \int_0^\infty \int_{\frac{x+\xi+a}{v_s}}^t \frac{\chi(\tau, \xi) e^{-2\eta(t-\tau)} d\tau d\xi}{\sqrt{v_s^2(t-\tau)^2 - (x+\xi+a)^2}} + \Delta T_B, \quad (60)$$

$$\Delta T_B(t, x) = \frac{2}{\pi} \int_0^\infty \int_{\frac{x+\xi+a}{v_s}}^t \chi(\tau, \xi) e^{-2\eta(t-\tau)} \Delta g(t-\tau, x, \xi)|_{q=1} d\tau d\xi, \quad (61)$$

where $\Delta g(t, x, \xi)$ is defined by Eq. (56). According to the analysis of the sudden point heat supply (see Sect. 6.3), neglecting the fast term in (56), i.e., putting $q = 0$, results in a loss in the accuracy of the solution for the kinetic temperature at and near the boundary. The steady-state non-equilibrium solution for kinetic temperature, if it exists, is defined as $T^\infty(x) \stackrel{\text{def}}{=} T(x, \infty)$. Note that the discrete-continuum solution for the kinetic temperature in the form is valid only for weakly dissipative case ($\eta \ll \omega_e$), while the symmetrical continuum solution is valid for arbitrary η . Note also that the expression for the kinetic temperature with the source, defined by Eq. (59) coincides with Eq. (54) at $\eta \rightarrow 0+$.

Consider the sudden point heat supply, which we define by the Dirac delta function, namely

$$\chi(t, x) = \chi^0 a \delta(x - \xi) H(t), \quad (62)$$

where χ^0 is a constant of K/s dimension. The corresponding expression for the source χ in the discrete form is written as

$$\chi_n(t) = \chi^0 \delta_{n,j} H(t). \quad (63)$$

The discrete solution for the kinetic temperature is obtained by substitution of Eq. (63) to Eq. (20) with taking into account (31) and dropping out the term $O(\eta/\omega_e)$, what yields

$$T_n(t) = 2\chi^0 \int_0^t e^{-2\eta\tau} (J_{2|n-j|}(2\omega_e\tau) + J_{2(n+j+1)}(2\omega_e\tau))^2 d\tau. \quad (64)$$

In the limit $t \rightarrow \infty$, the equation for T_n may be obtained in terms of the hypergeometric functions [76], in a closed but rather cumbersome form.

The symmetrical continuum solution is obtained by substitution of Eq. (62) to Eq. (27) yields

$$T(t, x) = \frac{\chi^0 a H(v_s t - |x - \xi|)}{\pi} \int_{\frac{|x-\xi|}{v_s}}^t \frac{e^{-2\eta\tau} d\tau}{\sqrt{v_s^2 \tau^2 - (x - \xi)^2}} + \frac{\chi^0 a H(v_s t - |x + \xi|)}{\pi} \int_{\frac{x+\xi}{v_s}}^t \frac{e^{-2\eta\tau} d\tau}{\sqrt{v_s^2 \tau^2 - (x + \xi)^2}}. \quad (65)$$

If the viscosity takes place, there is a nonequilibrium steady state, at which the symmetrical continuum solution has the following form:

$$T^\infty(x) = \frac{\chi^0}{\pi\omega_e} \left(K_0 \left(\frac{2\eta|x - \xi|}{v_s} \right) + K_0 \left(\frac{2\eta(x + \xi)}{v_s} \right) \right), \quad (66)$$

where K is the modified Bessel function of the second kind.

The discrete-continuum solution for the kinetic temperature is obtained by substitution of Eq. (62) to Eq. (60), what yields

$$T(t, x) = \frac{\chi^0 a H(v_s t - |x - \xi|)}{\pi} \int_{\frac{|x-\xi|}{v_s}}^t \frac{e^{-2\eta\tau} d\tau}{\sqrt{v_s^2 \tau^2 - (x - \xi)^2}} + \frac{\chi^0 a H(v_s t - |x + \xi + a|)}{\pi} \int_{\frac{x+\xi+a}{v_s}}^t \frac{e^{-2\eta\tau} d\tau}{\sqrt{v_s^2 \tau^2 - (x + \xi + a)^2}} + \Delta T_B, \quad (67)$$

$$\Delta T_B(t, x) = \frac{2\chi^0 a H(v_s t - |x + \xi + a|)}{\pi} \int_{\frac{x+\xi+a}{v_s}}^t e^{-2\eta\tau} \Delta g(\tau, \xi, x)|_{q=1} d\tau. \quad (68)$$

Therefore, the stationary solution, T^∞ , is written as

$$T^\infty(x) = \frac{\chi^0}{\pi\omega_e} \left(K_0 \left(\frac{2\eta|x - \xi|}{v_s} \right) + K_0 \left(\frac{2\eta(x + \xi + a)}{v_s} \right) \right) + \frac{2\chi^0 a}{\pi} \int_{\frac{x+\xi+a}{v_s}}^\infty e^{-2\eta\tau} \Delta g(\tau, \xi, x)|_{q=1} d\tau. \quad (69)$$

The principal difference of the steady-state solution for the kinetic temperature in the discrete-continuum and classical-continuum descriptions is the possibility to obtain a closed-form solution in the latter kind of description in contrast to the first one.

Now we find an approximate solution for the far field (for $x \gg \xi + a$) of kinetic temperature. Far from the boundary, the symmetrical continuum steady-state solution (Eq. (66)) may be estimated by using the following expansion of the modified Bessel function of the second kind at large argument (see Eq. 9.7.2 in [81]):

$$K_0(\lambda) = e^{-\lambda} \sqrt{\frac{\pi}{2\lambda}} (1 + O(\lambda^{-1})), \quad \lambda \rightarrow \infty. \quad (70)$$

Substitution of the first term in (70) to (66) yields

$$T^\infty(x) \approx \frac{\chi^0}{2\omega_e} \left(\sqrt{\frac{v_s}{\pi\eta(x - \xi)}} e^{-\frac{2\eta(x - \xi)}{v_s}} + \sqrt{\frac{v_s}{\pi\eta(x + \xi)}} e^{-\frac{2\eta(x + \xi)}{v_s}} \right), \quad x \rightarrow \infty. \quad (71)$$

Approximation of the far-field discrete-continuum solution implies asymptotic estimate of the last term in (69), ΔT_B . Instead of using well-known asymptotic techniques [82] we estimate (69) in easier way, knowing behavior of the function Δg . If the source is not at the boundary, then the Δg for $x \gg \xi + a$ represents an integral from the fast-oscillating function, because the characteristic frequencies of the incident and reflected thermal waves are not close to each other (see Sect. 5.2). Therefore, Δg may be neglected, and the expression for the far-field kinetic temperature is written as

$$T^\infty(x)|_{\xi \neq 0} \approx \frac{\chi^0}{2\omega_e} \left(\sqrt{\frac{v_s}{\pi\eta(x-\xi)}} e^{-\frac{2\eta(x-\xi)}{v_s}} + \sqrt{\frac{v_s}{\pi\eta(x+\xi+a)}} e^{-\frac{2\eta(x+\xi+a)}{v_s}} \right), \quad x \rightarrow \infty. \quad (72)$$

Thus, for $\xi \neq 0$ the far-field discrete-continuum solution does not sufficiently differ from the far-field symmetrical continuum solution (71). For $\xi = 0$, the estimation (72) is not valid, because the last term in (69) may not be negligible. However, we neglect fast-oscillating terms in Δg , substituting $q = 0$. Simplifying Eq. (56) by using Eq. (34), we write the following expression for ΔT_B :

$$\Delta T_B \approx \frac{2\chi^0 a}{\pi} \int_{\frac{x+a}{v_s}}^{\infty} \frac{e^{-2\eta\tau} \left(-1 + \frac{(2x+a)^2}{2v_s^2\tau^2} \right) d\tau}{\sqrt[4]{(v_s^2\tau^2 - x^2)(v_s^2\tau^2 - (x+a)^2)}}. \quad (73)$$

Put in the integral in (73) $\tilde{\tau} = \tau - \frac{x+a}{v_s}$. Then, (73) is rewritten as

$$\Delta T_B \approx \frac{2\chi^0 a}{\pi} e^{-\frac{2\eta(x+a)}{v_s}} \int_0^{\infty} \frac{e^{-2\eta\tilde{\tau}} \left(-1 + \frac{(2x+a)^2}{2(v_s\tilde{\tau}+x+a)^2} \right) d\tilde{\tau}}{\sqrt[4]{((v_s\tilde{\tau}+x+a)^2 - x^2)((v_s\tilde{\tau}+x+a)^2 - (x+a)^2)}}. \quad (74)$$

Expanding the integrand in (74) at $x = \infty$ neglecting the terms of order of $x^{-\frac{3}{2}}$ and higher, and, using the identity

$$\int_0^{\infty} \frac{e^{-2\eta t} dt}{\sqrt[4]{v_s t(v_s t + a)}} = \sqrt[4]{\frac{2a}{v_s^3\eta}} \frac{e^{\frac{\eta}{\omega_e}} \sqrt{\pi} K_{\frac{1}{4}} \left(\frac{\eta}{\omega_e} \right)}{\Gamma\left(\frac{1}{4}\right)}, \quad (75)$$

where $\Gamma(y) \stackrel{\text{def}}{=} \int_0^{\infty} e^{-t} t^{y-1} dt$ is the Gamma function, we have

$$\Delta T_B \approx \frac{\sqrt[4]{8}\chi^0 a}{\sqrt{\pi}\Gamma\left(\frac{1}{4}\right)} \sqrt[4]{\frac{a}{v_s^3\eta}} K_{\frac{1}{4}} \left(\frac{\eta}{\omega_e} \right) e^{-\frac{\eta}{\omega_e}} \frac{e^{-\frac{2\eta x}{v_s}}}{\sqrt{x}}, \quad x \rightarrow \infty. \quad (76)$$

Therefore, the expression for the far-field kinetic temperature at the source at the boundary has the form

$$T^\infty(x)|_{\xi=0} \approx \frac{\chi^0}{2\omega_e} \left(\left(\sqrt{\frac{v_s}{\eta}} + \frac{2}{\Gamma\left(\frac{1}{4}\right)} \sqrt[4]{\frac{8v_s a}{\eta}} K_{\frac{1}{4}} \left(\frac{\eta}{\omega_e} \right) e^{-\frac{\eta}{\omega_e}} \right) \frac{e^{-\frac{2\eta x}{v_s}}}{\sqrt{\pi x}} + \sqrt{\frac{v_s}{\pi\eta(x+a)}} e^{-\frac{2\eta(x+a)}{v_s}} \right), \quad x \rightarrow \infty. \quad (77)$$

Thus, we have obtained analytical solution for the kinetic temperature in the continuum limit. The closed-form solution has been managed to be obtained only either for the special cases, (point heat pulse and point heat supply in the limit $\eta \rightarrow 0+$), or for estimation of the stationary field of the kinetic temperature far from the boundary.

6 Discussion of results

In this section, we compare the analytical results corresponding to the discrete and continuum solutions for the kinetic temperature with the results of the numerical solution. Since we study different types of heat supply, the details of the numerical simulations for each type are discussed separately.

6.1 Point heat pulse

Consider the point heat pulse, defined by Eq. (59). We compare analytical results for the kinetic temperature, corresponding to the discrete solution (Eq. (42)), symmetrical continuum solution¹³ (Eq. (49)), and continuum solution (Eq. (51)) with the corresponding numerical solution. The latter is obtained by the integration of Eqs. (29) with the initial conditions (30) using the symplectic leap-frog method with a time step $\omega_e t = 0.02$. The comparison is shown in Figs. 1, 2.

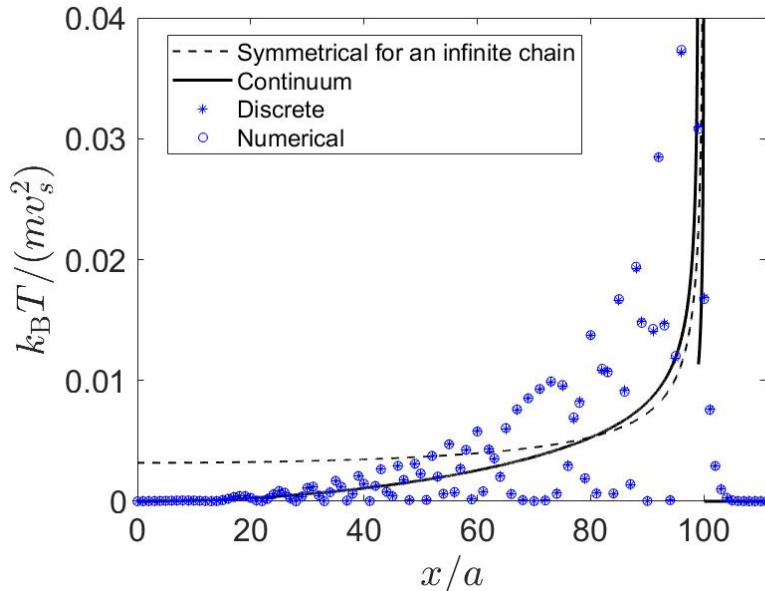


Figure 1: Kinetic temperature in the semi-infinite chain undergone point heat pulse at $j = 0$. Comparison of analytical and numerical solutions is shown at $\omega_e t = 100$. The continuum, symmetrical continuum and discrete solutions (Eqs. (51), (49) and (42) respectively) are demonstrated.

It is seen in Fig. 1 that the symmetrical continuum solution inadequately describes propagation of thermal waves. The latter is well-described by the continuum solution, which looks like a spatial average of the discrete solution. As expected, pulse far outside the boundary changes the kinetic temperature field in the neighborhood of the $n = 0$ only due to the anti-localization of thermal waves is significantly weaker in contrast to the case of pulse at the boundary (this is seen well from the expression (48)). The fast decay of the continuum solution at the boundary associated with the anti-localization of thermal waves is demonstrated in Fig. 3.

6.2 Rectangular and step heat pulses

Consider a rectangular heat pulse, defined as

$$k_B T^0(x) = m v_s^2 (H(x - L_1) - H(x - L_1 - L_2)), \quad (78)$$

where L_1 is a distance from the boundary to the perturbation; L_2 is a width of perturbation. Consider also a step heat pulse, defined as

$$k_B T^0(x) = m v_s^2 H(L - x), \quad (79)$$

¹³Although the source of the heat pulse does not obey the condition of its continuity at a distance of order at least two dozen particles, we consider the solution pertinent for comparison with the continuum solution.

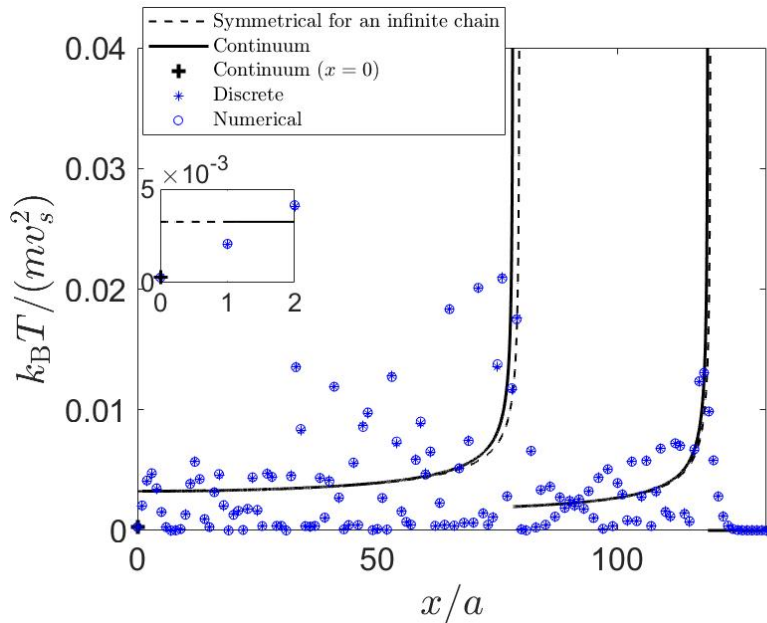


Figure 2: Kinetic temperature in the semi-infinite chain undergone point heat pulse at $j = 20$. Comparison of analytical and numerical solutions is shown at $\omega_e t = 100$. The continuum, symmetrical continuum and discrete solutions (Eqs. (51), (49) and (42) respectively) are demonstrated.

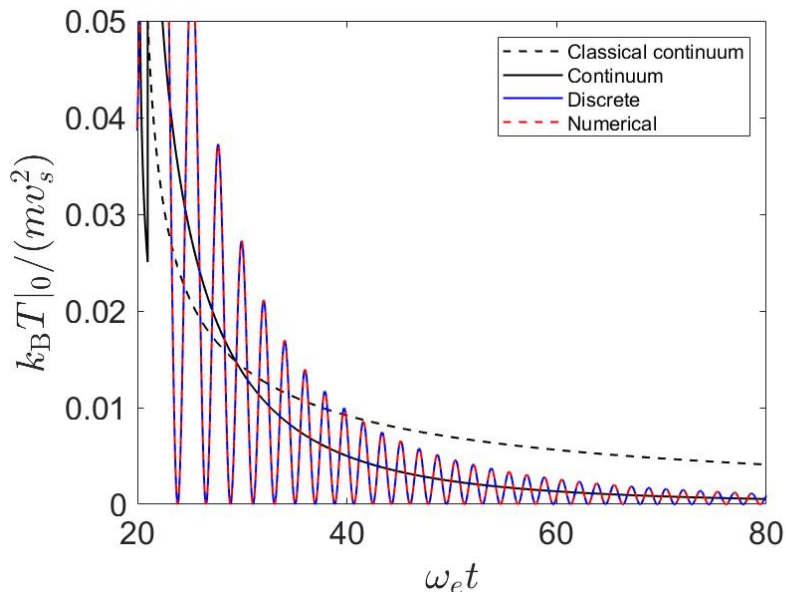


Figure 3: Evolution in of the kinetic temperature at the boundary after heat pulse at the point $j = 20$. The continuum, symmetrical continuum and discrete solutions (Eqs. (51), (49) and (42) respectively) are demonstrated.

where L is a width of perturbation. We compare analytical results for the kinetic temperature, corresponding to the discrete solution (Eq. (40)), symmetrical continuum solution (Eq. (58)), discrete-continuum solution (Eqs. (54), (55) and continuum solution (Eqs. (54), (57)) with the corresponding numerical solutions. The latter is obtained in the way described in Sect. 5 in [35]. To obtain the expression for the kinetic temperature, corresponding to the continuum and discrete-continuum solution, the integrals in Eqs. (54), (57) are calculated by using the Clenshaw-Curtis quadrature. The comparison of the analytical and numerical solutions

is shown in Figs. 4, 5. It is seen in Figs. 4, 5 that the discrete-continuum and continuum

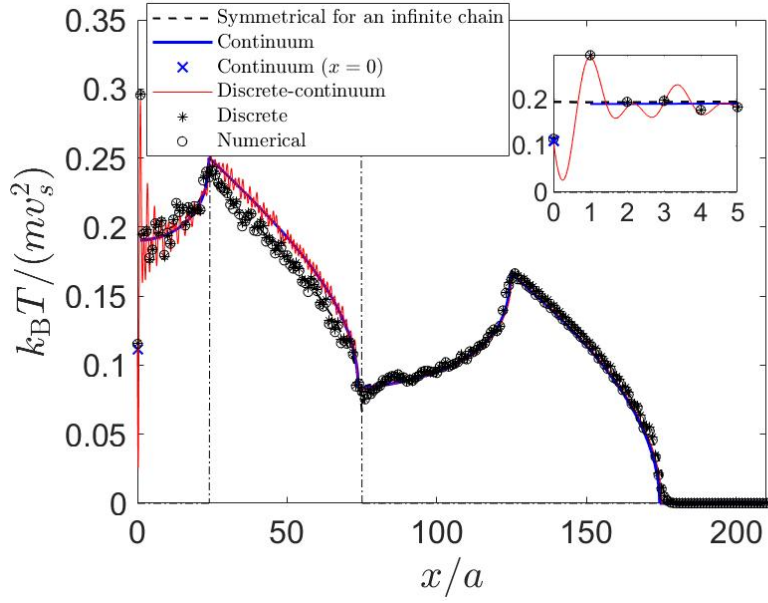


Figure 4: Kinetic temperature in the semi-infinite chain undergone rectangular perturbation (78) at $\omega_e t = 100$. Width of the initial thermal perturbation is shown by the dash-dotted lines. The continuum (Eqs. (54), (57)), discrete-continuum (Eqs. (54), (55)), symmetrical continuum (Eq. (58)) and discrete (Eq. (40)) solutions are demonstrated.

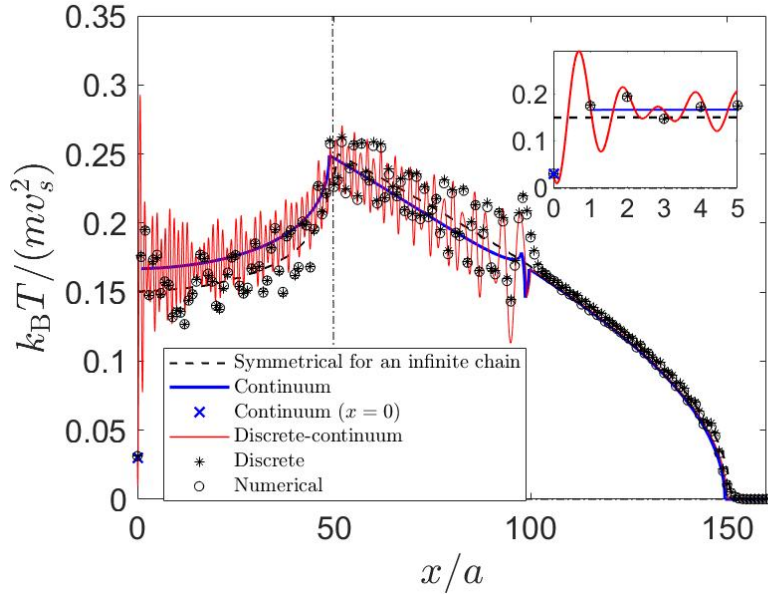


Figure 5: Kinetic temperature in the semi-infinite chain undergone step perturbation (79) at $\omega_e t = 100$. Width of the initial thermal perturbation is shown by the dash-dotted line. The continuum (Eqs. (54), (57)), discrete-continuum (Eqs. (54), (55)), symmetrical continuum (Eq. (58)) and discrete (Eq. (40)) solutions are demonstrated.

solutions describe the kinetic temperature at boundary more accurately than the symmetrical continuum one. Nevertheless, in the domain of initial perturbation, the discrete-continuum and continuum solutions deviate from the exact (discrete) numerical solutions (see Figs. 4, 5) and

also from the symmetrical continuum solution, which coincides with these in Fig. 4. The reason of raised discrepancies is that, apparently, the symmetrical continuum solution contains the term $\frac{T^0(x)}{2}J_0(4\omega_e t)$, corresponding to the local (in the domain of perturbation) equilibration between the kinetic and potential energies. Derivation of the continuum solution has been implied to neglect terms, corresponding to the fast motions of the incident and reflected thermal waves (first two terms in Eq. (37)). Since the first term in Eq. (58) decays in time, the symmetrical continuum solution is expected to gradually coincide with the continuum and discrete-continuum ones. It is seen in Fig. 5 that step perturbation leads to more pronounced oscillations of the kinetic temperature, which are described by the discrete and discrete-continuum solutions. From the comparison of the continuum and discrete-continuum solutions we conclude that a perturbation, propagating approximately with the speed of sound (which was for the first time detected in [35]), is an artefact, described by the ΔT_B (namely, the main contribution is given by the first term in the numerator of Eq. (56)), determined in Eq. (55).

Remark 6. Note that profiles of the continuum and symmetrical continuum kinetic temperature have breaks in zone of fronts and boundaries of initial perturbation (see Figs. 4, 5). It means that spatial derivation of the kinetic temperature is discontinuous at the corresponding points. Perturbation of inclined step or rectangular profile is expected to fix this drawback (see [39]).

Evolution of the kinetic temperature at the boundary is shown in Figs. 6,7. It is seen in

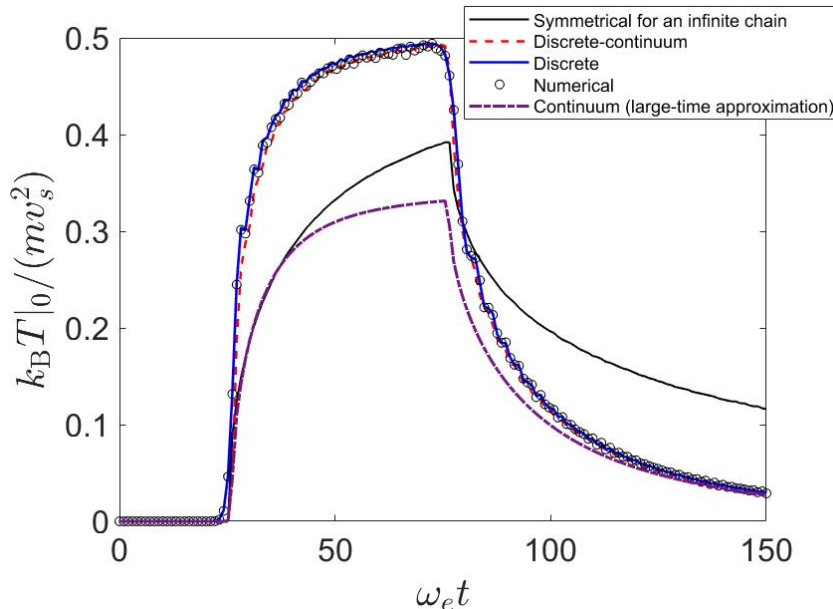


Figure 6: Kinetic temperature in the semi-infinite chain undergone rectangular perturbation (78) at $\omega_e t = 100$. The width of the initial thermal perturbation is shown by the dash-dotted line. The continuum (Eqs. (54), (57)), discrete-continuum (Eqs. (54), (55)), symmetrical continuum (Eq. (58)) and discrete (Eq. (40)) solutions are demonstrated.

Figs. 6, 7 that, in continuum limit, evolution of the kinetic temperature at the boundary is adequately described by the discrete-continuum and continuum solutions. However, the latter solution describes the evolution of the kinetic temperature at large times only after reflection of the thermal wave. The discrete-continuum solution takes into account the fast processes associated with interactions with incident and reflected waves. Note also that the continuum solution looks like a spatial average of a discrete solution (see Figs. 6,7).

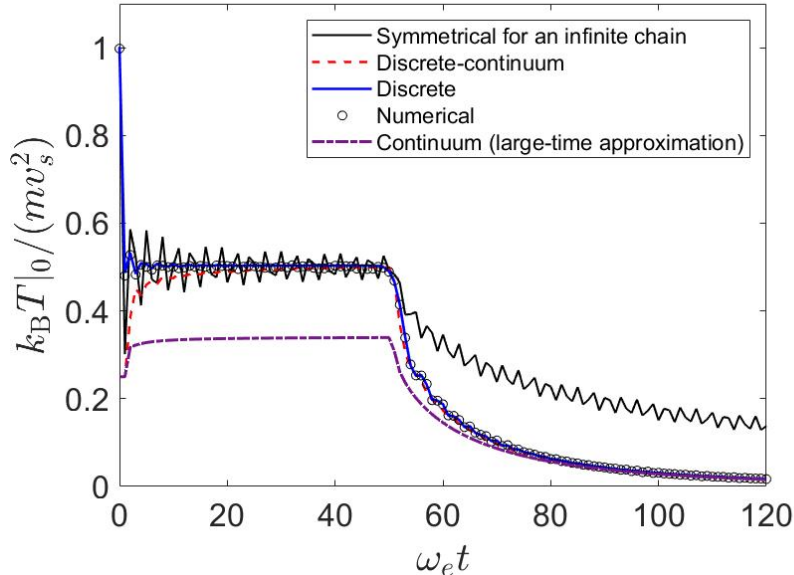


Figure 7: Kinetic temperature in the semi-infinite chain undergone step perturbation (79) at $\omega_e t = 100$. The width of the initial thermal perturbation is shown by the dash-dotted line. The continuum (Eqs. (54), (57)), discrete-continuum (Eqs. (54), (55)), symmetrical continuum (Eq. (58)) and discrete (Eq. (40)) solutions are demonstrated.

6.3 Point heat supply with constant intensity

Consider the point heat supply, defined by Eq. (62) in the continuum form and by Eq. (63) in the discrete one. We compare analytical results for the kinetic temperature, corresponding to the discrete Eq. (64) and continuum solutions (65), (69), (72), (77) with the corresponding numerical solutions. Details of the numerical simulations are discussed in the Appendix C. The integrals, in which the analytical solution consists, are calculated using the trapezoidal rule. In particular, the steady-state solution for the dissipative case is obtained as the non-stationary one for a sufficiently long time after the beginning of the supply (we take $\omega_e t = 500$). Analytical calculations are performed using Taichi software to accelerate them. Here, we investigate the obtained results, corresponding to the supply at both the point outside the boundary (for instance, $j = 5$) and at the boundary.

6.3.1 The non-dissipative case

We consider the non-dissipative case ($\eta \rightarrow 0+$). Then, the symmetrical continuum solution for the kinetic temperature has the form:

$$T(t, x) = \frac{\chi^0 H(v_s t - |x - \xi|)}{\pi \omega_e} \ln \frac{v_s t + \sqrt{v_s^2 t^2 - (x - \xi)^2}}{|x - \xi|} + \frac{\chi^0 H(v_s t - (x + \xi))}{\pi \omega_e} \ln \frac{v_s t + \sqrt{v_s^2 t^2 - (x + \xi)^2}}{x + \xi}, \quad (80)$$

from which logarithmic growth of $T(t, x)$ follows. In turn, the discrete-continuum solution is obtained by substitution of $\eta = 0$ to Eq. (67), what yields to coincidence of the first two terms, denoting the contributions from incident and reflected waves with Eq. (80), where $x + \xi$ is replaced by $x + \xi + a$. The discrete solution is obtained by substitution of $\eta = 0$ to Eq. (64).

We study the evolution in time of the kinetic temperature and the influence of the free boundary of the latter. Consider the kinetic temperature at the boundary. The comparison of analytical and numerical solutions for the latter is shown in Fig. 8.

We see that, at short times, the discrete and discrete-continuum solutions for the kinetic

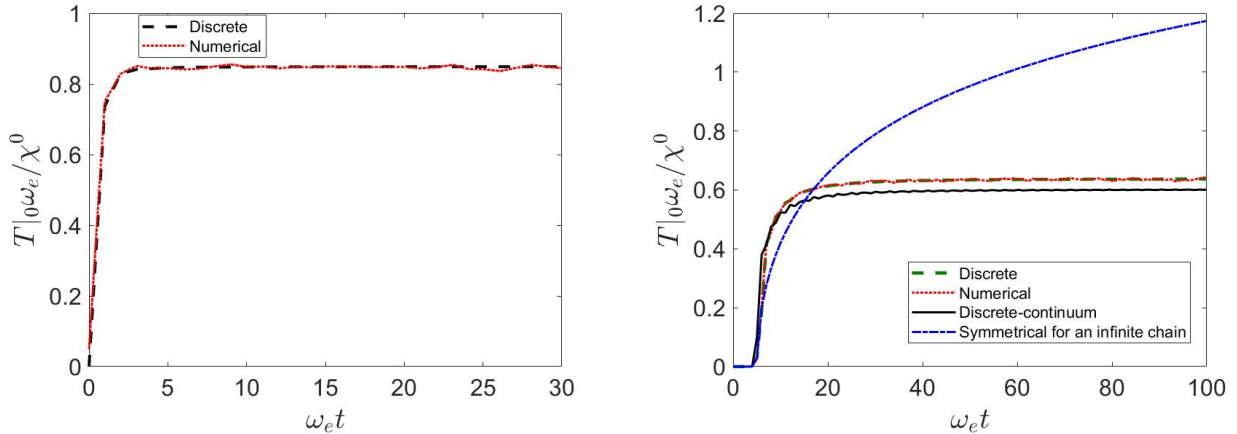


Figure 8: Evolution of the kinetic temperature at the boundary in the semi-infinite chain undergone heat supply at the point $j = 0$ (left) and $j = 5$ (right) in the non-dissipative case ($\eta \rightarrow 0+$). The discrete (64), discrete-continuum (Eqs. (60), (61)) and symmetrical continuum (Eq. (80)) solutions are demonstrated.

temperature at the boundary grow faster than the symmetrical continuum one (see Fig. 8B). However, at large times, growth of the discrete solution slows down sufficiently insomuch that they seem to tend to the stationary values. To explain the reason for this behavior of these solutions and determine whether the corresponding process is a transition to the local stationary state or an anomalously slow growth of the kinetic temperature, we investigate the discrete-continuum solution, which behaves significantly similar to the discrete one, although their stationary values at large times differ (see Fig. 8B). We analyze the dependence of the first two terms in Eq. (67), which is shown in Fig. 9. We see that, firstly, after the incident thermal

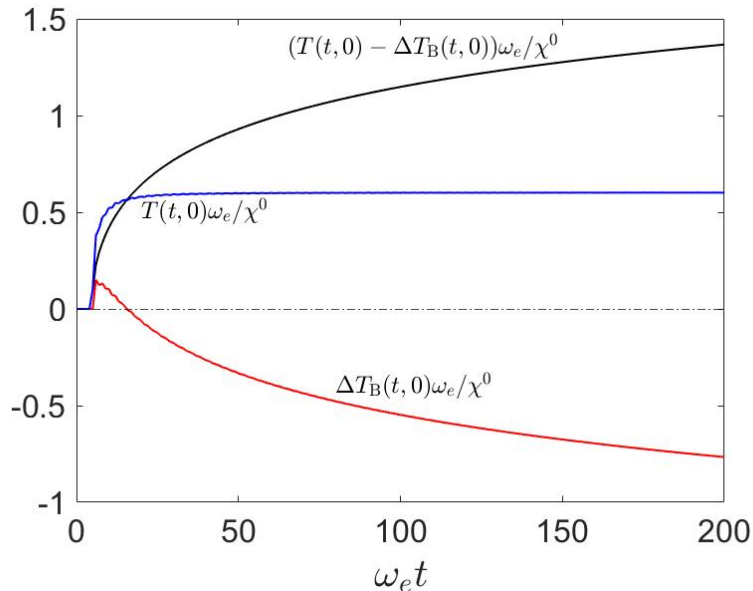


Figure 9: Dependence of the discrete-continuum solution (Eqs. (60), (61)) for the kinetic temperature (blue line), ΔT_B (red line) and sum of the contributions from the incident and reflected waves (black line) are shown.

wave reaches the boundary, the discrete-continuum solution for the kinetic temperature grows faster than the sum of its contribution from the incident and reflected waves due to $\Delta T_B > 0$.

Secondly, the growth of the kinetic temperature stops exactly at the moment of time, when the function ΔT_B changes the sign. At large times, the absolute value of $\Delta T_B > 0$ grows in time similarly to the sum of the aforementioned contributions. From the analysis of the time derivatives of this sum and ΔT_B we conclude that their absolute change rate is equal to each other, and therefore the kinetic temperature becomes *constant* in time. The negative change in the kinetic temperature at the boundary is caused by the interactions of incident and reflected waves; that is, it shares the same reason as the anti-localization of the thermal wave at the boundary in the case of instantaneous heat perturbation. (see Sects. 5.3.1, 5.3.2). According to the preliminary results, firstly, the stationary state is observed at the points between the boundary and the heat supply points (if these are not coincide). Secondly, the kinetic temperature at the boundary does not grow in time regardless of the point of heat supply.

The profiles of the kinetic temperature at fixed moment of time are shown ¹⁴ in Fig. 10. It is seen in Fig. 10 that, when the supply occurs at the point $j = 0$, the kinetic temperature

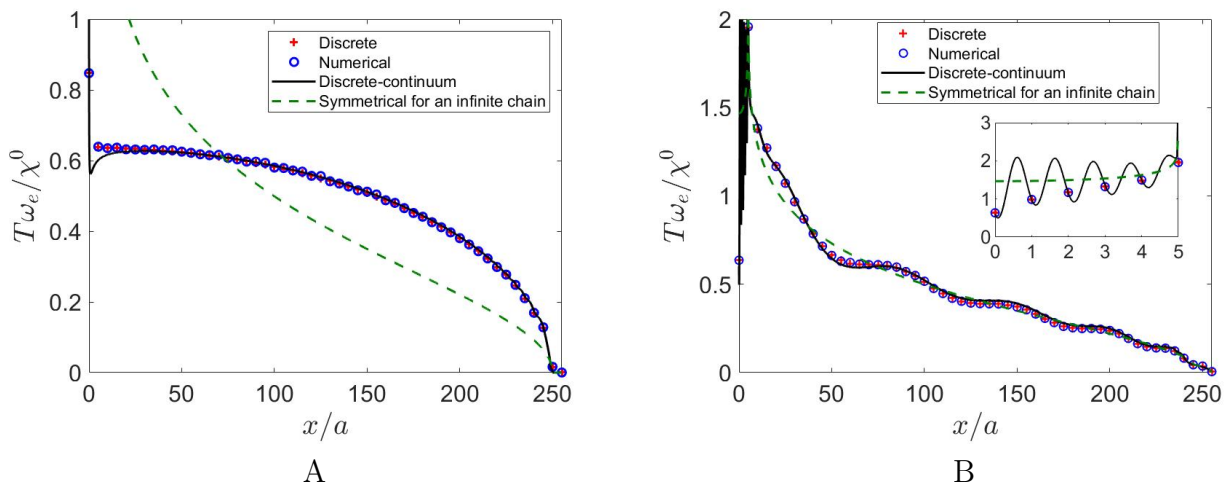


Figure 10: Profiles of the kinetic temperature at the boundary in the semi-infinite chain undergone heat supply at the point $j = 0$ (A) and $j = 5$ (B) at $\omega_e t = 250$ in the non-dissipative case ($\eta \rightarrow 0+$). The discrete (64), discrete-continuum (Eqs. (60), (61)) and symmetrical continuum (Eq. (80)) solutions are demonstrated.

at the points far from the boundary grows sufficiently slower, than in the case of supply at the point $j = 5$. In order to ensure the latter, we investigate the evolution of the kinetic temperature at the arbitrary point far from the boundary. Comparison of the corresponding solutions is shown in Fig. 11. It is seen that, in the case of the supply at the point $j = 0$, the kinetic temperature far from the boundary does not grow at large times and tends to some stationary value (see Fig. 11A), in contrast to the kinetic temperature in the case of supply outside the boundary (see Fig. 11B). Having analyzed (in the similar way) behavior of the kinetic temperature at several points, we conclude that the heat supply at the boundary results in the non-equilibrium stationary state, becoming gradually at *all* heated points. From Figs. 8, 10, 11 it is seen that heat transport is adequately described by the discrete and discrete-continuum solutions ¹⁵. Thus, the symmetrical continuum solution is inapplicable.

¹⁴To avoid a jumble of symbols in Fig. 10, we plot the discrete and numerical solutions not at every point, but rather at every fifth.

¹⁵Adequateness of the discrete-continuum description takes a place, despite a property of the corresponding solution to be non-monotonic between the points near the boundary (see Fig. 10B, inlet). The details are discussed in Sect. 7

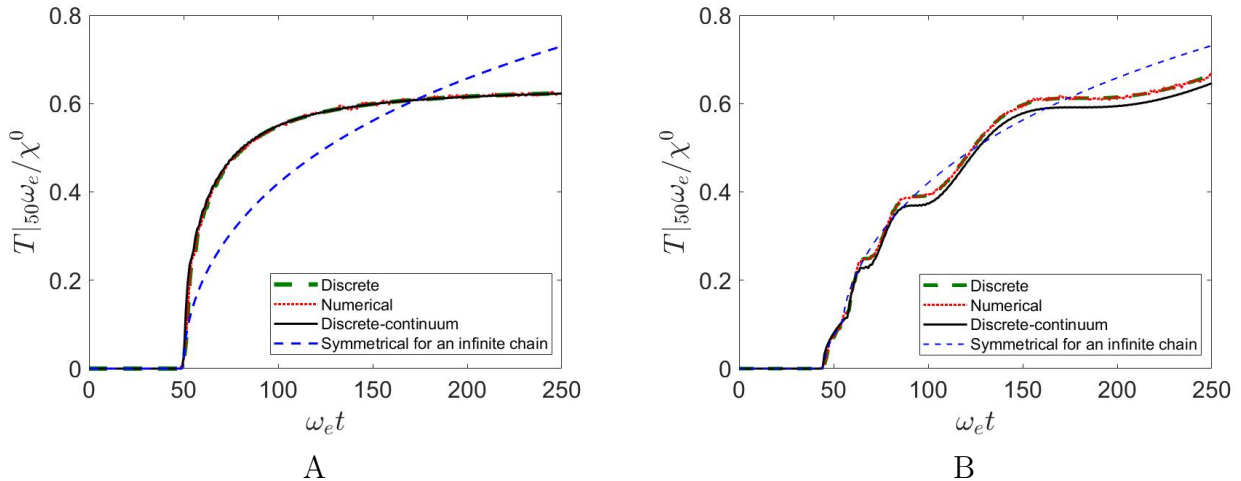


Figure 11: Evolution of the kinetic temperature at the 50-th point in the semi-infinite chain undergone heat supply at the point $j = 0$ (A) and $j = 5$ (B) in the non-dissipative case ($\eta \rightarrow 0+$). The discrete (64), discrete-continuum (Eqs. (60), (61)) and symmetrical continuum (Eq. (80)) solutions are demonstrated.

6.3.2 The dissipative case

In the dissipative case, the transition to the nonequilibrium steady state is expected at all points. The kinetic temperature as a function of time tends to some stationary value (according to Eq. (64)). Since the behavior of the kinetic temperature function at the fixed points is similar to that of one in the non-dissipative case (although the stationary value is, obviously, less due to the viscosity), considering the stationary solution is of interest. The solutions for the kinetic temperature, corresponding to the in the case of the supply at the point $j = 5$ is shown in Fig. 12. We see that, firstly, far from the boundary the discrete-continuum and symmetrical continuum solution for the kinetic temperature are in a good agreement. However, near the boundary, the discrete-continuum solution describes the kinetic temperature field more accurately than the continuum solution, although the difference between the solutions is not sufficient. The far-field asymptotic solution (72) describes the kinetic temperature field (both the discrete-continuum and continuum solutions) rather accurately for $x/a > 30$. The other situation is when the supply is at the boundary (see Fig. 13). We see that behavior of the symmetrical continuum solution for the stationary field of the kinetic temperature is even qualitatively different than behavior of the discrete-continuum solution. In contrast to the case of supply at the point outside the boundary, the qualitative difference of the solution is observed not only near the boundary but everywhere. The far-field asymptotic solution (77) describes the kinetic temperature field rather accurately for $x/a > 60$. One can observe in Fig. 13, that, near the boundary, the discrete and discrete-continuum solutions change more abruptly than the symmetrical continuum solution. We cannot provide a convincing explanation for the latter observation.

7 Conclusions

In this paper, heat transport in a semi-infinite free end chain lying in a weakly viscous environment and having an arbitrary heat source has been investigated. We started with Eqs. (1) for the stochastic dynamics of the chain and derived the exact expression for the kinetic temperature (Eq. (19)), the simplified version of which for the weakly dissipative case (Eq. (20)) is referred to as the discrete solution. Continualization of the latter is performed in two ways.

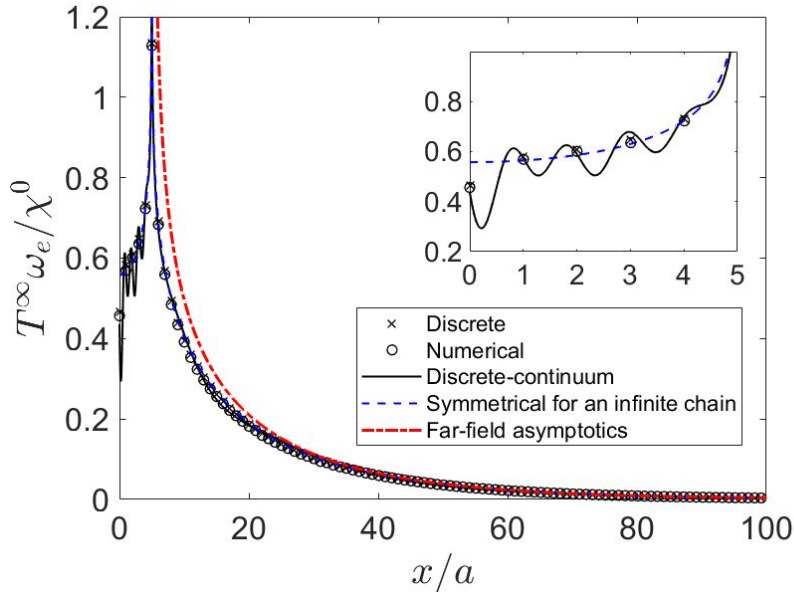


Figure 12: Stationary field of the kinetic temperature in the semi-infinite Hooke chain undergone sudden heat supply at the point $j = 5$. The discrete (64), discrete-continuum (Eqs. (60), (61)) and symmetrical continuum (Eq. (65)) solutions and far-field asymptotics (72) are demonstrated. The calculations are performed for $\eta/\omega_e = 0.02$.

The first is to apply the principle of symmetry of the continuum solution, formulated in [35], to the continuum solution for the kinetic temperature in the infinite chain, obtained in [32]. The obtained solution is termed a symmetrical continuum solution. The second way is through the estimate of the fundamental thermal solution at the fronts of the incident and reflected waves at $t \rightarrow \infty$, which yields the sum of the contributions of the incident and reflected waves to the expression for the kinetic temperature and an additional crossed term. Depending on whether we include the fast term of the latter in the expression for the kinetic temperature, we define this to be either a continuum solution or a discrete-continuum one. If this fast term is not included (for the continuum fundamental solution in the case of a heat pulse), then we call the obtained solution continuum. In the case of sudden point heat supply and a heat pulse of wide profile, the fast term should be included, and then we call the obtained solution discrete-continuum. By asymptotic analysis of the continuum fundamental solution, we revealed that instantaneous heat supply, i.e., a heat pulse of any initial temperature profile, leads to a rapid decay (as $1/t^3$) of the kinetic temperature at the boundary. This is the anti-localization (this phenomenon was introduced in [42]) of the reflected wave. It explains the mismatch of the kinetic temperature profiles corresponding to the discrete and symmetrical continuum solutions at and near the boundary, an explanation of which was not provided in [35]. The closer to the boundary the source of the heat pulse is, the stronger the anti-localization is. In the case of sudden point heat supply, the transition to the non-equilibrium steady state is shown to take place even in the non-dissipative case (near the boundary during supply at the point out of it and everywhere during supply at the boundary) for the same reason as the anti-localization after a heat pulse. It is described quite well by the obtained discrete-continuum solution in contrast to the classical-continuum one, according to which the kinetic temperature always grows in time. The only one which the classical-continuum solution describes correctly is the stationary far field of the kinetic temperature in the dissipative case, when the heat source is out from the boundary.

Despite the fact that continuum and discrete-continuum solutions describe the process of heat transport in the chain quite accurately, they have the following drawbacks. The first

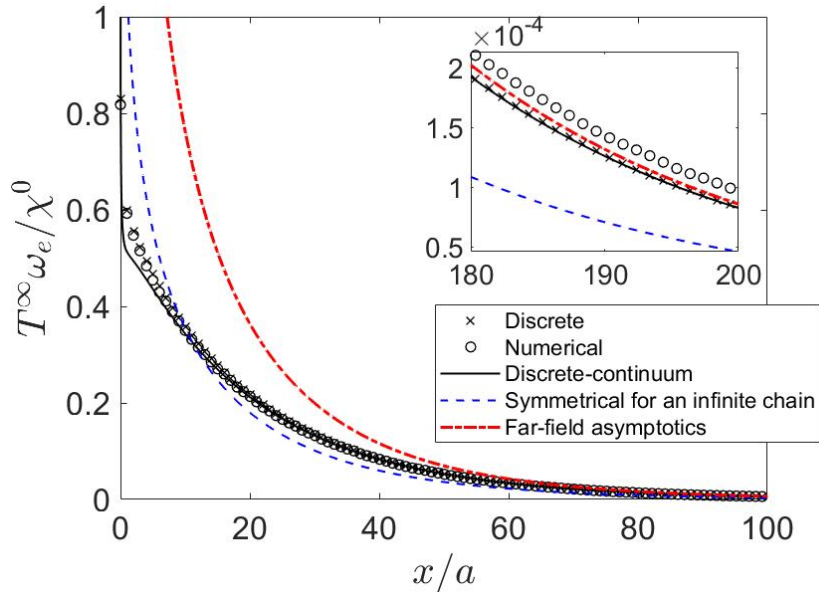


Figure 13: Stationary field of the kinetic temperature in the semi-infinite Hooke chain undergone sudden heat supply at the point $j = 0$. The discrete (64), discrete-continuum (Eqs. (60), (61)) and symmetrical continuum (Eq. (65)) solutions and far-field asymptotics (77) are demonstrated. The calculations are performed for $\eta/\omega_e = 0.02$.

is singularity: the continuum fundamental solution is singular at the fronts and the discrete-continuum solution is singular at the point of heat supply. We have no rational idea how to fix this drawback. We tried to replace the source, described by the Dirac delta function (Eq. (62)), with one described by the Gaussian function with a width equal to a . This idea has not produced a convincing result. We assume that singularities, encountered both in the considered problem and also in [32, 34, 47], could be eliminated by using the theory of analysis of nonlocal functions, proposed in [83]. The second drawback is the oscillation-type behavior of the discrete-continuum solution between the particle points (especially as it manifests near the boundary during the constant intensity heat supply). Although this drawback does not affect the nature of heat propagation itself, it can be seriously manifested when the discrete-continuum solution is used as a constitutive relation in thermoelastic or thermoelectromagnetic problems.

In our opinion, the following generalizations are made from the results of the paper. Firstly, it is a solution to the problem considered in the paper with respect to the heat flux. Secondly, it would be interesting to consider a third way of continualization of the discrete solution (20) by using the quasicontinuum description, according to [88, 89], and to compare the result for the kinetic temperature with the one obtained as proposed in Sect. 5.2. Thirdly, the approaches proposed in this paper can be generalized to more complicated one-dimensional systems (e.g., having an additional elastic substrate, damper elements, two or more sublattices) or in high-dimensional lattices. For the latter, the developed theory of (quasi-)ballistic heat transport in the high-dimensional lattices, in particular, might be helpful for a more clarified description of phonon focusing than the one given by the continuum theory [84, 85, 86]. Finally, the theory of energy supply into the semi-infinite chain, presented in this paper and in [90], is expected to be useful for the analysis of heat transport problems, composed of two dissimilar homogeneous semi-infinite chains (i.e., in a composite chain).

8 Acknowledgements

Information about funding will be added later. The author thanks V.A. Kuzkin, A.M. Krivtsov, S.N. Gavrilov, E.V. Shishkina, A.A. Sokolov, E.F. Grekova and Jie Chen for valuable discussions.

A Derivation of Eq. (13)

Make the following change of variable in Eq. (9):

$$\mathbf{y} = e^{-\mathbf{A}t} \hat{\mathbf{u}}. \quad (81)$$

Then, to find $d\mathbf{y}$, we use the Itô lemma (see Eq. (6.12) in [87]). For the s -th component of $d\mathbf{y}$ it can be written as

$$dy_s = \left(\frac{\partial y_s}{\partial t} + \frac{\partial y_s}{\partial \hat{u}_\alpha} (\mathbf{A}\hat{\mathbf{u}})_\alpha + \frac{1}{2} \frac{\partial^2 y_s}{\partial \hat{u}_\alpha \partial \hat{u}_\beta} B_{\alpha\gamma} B_{\beta\gamma} \right) dt + \frac{\partial y_s}{\partial \hat{u}_\alpha} B_{\alpha\gamma} dW_\gamma, \quad (82)$$

where summation over repeating indices is implied ($\sum_\alpha X_\alpha Y_\alpha$). Substituting of each component of \mathbf{y} from Eq. (81) to Eq. (82) one conclude the first term of Eq. (82) to be equal to zero $\forall s$. Therefore, we have the following equation:

$$d\mathbf{y} = e^{-\mathbf{A}t} \mathbf{B} d\mathbf{W}, \quad (83)$$

whereas, due to the initial condition (12)

$$\mathbf{y} = \int_0^t e^{-\mathbf{A}\tau} \mathbf{B}(\tau) d\mathbf{W}. \quad (84)$$

The reverse substitution $\hat{\mathbf{u}} \rightarrow \mathbf{y}$ yields Eq. (9).

B Derivation of Eq. (16)

Substitution of Eq. (13) to Eq. (15) yields

$$\begin{aligned} \langle \hat{\mathbf{u}}_1 \otimes \hat{\mathbf{u}}_2 \rangle &= \left\langle \int_0^t \int_0^t \left(e^{\mathbf{A}_1(t-\tau_1)} \mathbf{B}_1(\tau) d\mathbf{W}_1 \right) \otimes \left(e^{\mathbf{A}_2(t-\tau_2)} \mathbf{B}_2(\tau) d\mathbf{W}_2 \right) \right\rangle \\ &= \left\langle \int_0^t \int_0^t e^{\mathbf{A}_1(t-\tau_1)} \mathbf{B}_1(\tau_1) d\mathbf{W}_1 \otimes \left(\mathbf{B}_2(\tau_2) d\mathbf{W}_2 \right) e^{\mathbf{A}_2^\top(t-\tau_2)} \right\rangle. \end{aligned} \quad (85)$$

Here, the property of transposition of the matrix exponent [91]

$$(e^{\mathbf{A}})^\top = e^{\mathbf{A}^\top}. \quad (86)$$

is used. We write the expression for dyadic product of the vectors in Eq. (85) as

$$\mathbf{B}_1(t_1) d\mathbf{W}_1 \otimes \left(\mathbf{B}_2(t_2) d\mathbf{W}_2 \right) = \begin{pmatrix} 0 & 0 \\ 0 & dg_{1,2} \end{pmatrix}, \quad (87)$$

$$\begin{aligned} dg_{1,2} &\stackrel{\text{def}}{=} \sum_{n,n'=0}^{\infty} b_n(t_1) b_{n'}(t_2) \cos \frac{(2n+1)\theta_1}{2} \cos \frac{(2n'+1)\theta_2}{2} dW_{n,1} dW_{n',2} \\ &= dt \sum_{n,n'=0}^{\infty} b_n(t_1) b_{n'}(t_2) \cos \frac{(2n+1)\theta_1}{2} \cos \frac{(2n'+1)\theta_2}{2} \rho_n(t_1) \rho_{n'}(t_2) \end{aligned} \quad (88)$$

By using the uncorrelatedness of the random variables (see Sect. 3 and Eq. (1)), we transform Eq. (85) to the form:

$$\langle \hat{\mathbf{u}}_1 \otimes \hat{\mathbf{u}}_2 \rangle = \int_0^t e^{A_1(t-\tau)} \mathbf{G}(\tau) e^{A_2^\top(t-\tau)} d\tau, \quad \mathbf{G}(t) \stackrel{\text{def}}{=} \begin{pmatrix} 0 & 0 \\ 0 & \sum_{n=0}^{\infty} b_n^2(t) \cos \frac{(2n+1)\theta_1}{2} \cos \frac{(2n+1)\theta_2}{2} \end{pmatrix}. \quad (89)$$

We see that the matrix \mathbf{G} is equal to the product $\mathbf{B}_1 \mathbf{B}_2^\top$, what proves Eq. (16). For a more rigorous derivation of the variance matrix, corresponding to the stochastic matrix equation in a form of Eq. (9), we recommend to look at Sect. 6.4. in [87].

C Details of numerics, related to Sect. 6.3

The numerical simulations yielding the results of Sect. 6.3 sufficiently differ from the case of a heat pulse. Therefore, we provide the details of these below.

We consider the chain with N particles¹⁶ and two free ends. Following [32], introduce the following dimensionless values:

$$\begin{aligned} \tilde{u} &\stackrel{\text{def}}{=} u/a, & \tilde{v} &\stackrel{\text{def}}{=} v/v_s, \\ \tilde{b} &\stackrel{\text{def}}{=} b/(v_s \sqrt{\omega_e}), & \tilde{\eta} &\stackrel{\text{def}}{=} \eta/\omega_e, \\ \tilde{t} &\stackrel{\text{def}}{=} \omega_e t, & \tilde{T} &\stackrel{\text{def}}{=} k_B T / (m v_s^2). \end{aligned} \quad (90)$$

Then, taking into account Eq. (63), we rewrite Eqs. (1) in a form

$$\begin{aligned} d\tilde{u}_n &= \tilde{v}_n d\tilde{t}, \quad n = 0, 1, \dots, N-1, \\ d\tilde{v}_n &= F_n d\tilde{t} + \tilde{b} \delta_{n,j} \rho_j \sqrt{d\tilde{t}}, \quad F_n(\tilde{u}_n, \tilde{v}_n) \stackrel{\text{def}}{=} (\tilde{u}_{n+1} - \tilde{u}_n) - (\tilde{u}_n - \tilde{u}_{n-1})(1 - \delta_{n,0}) - 2\tilde{\eta} \tilde{v}_n, \end{aligned} \quad (91)$$

with zero initial conditions with respect to the dimensionless particle displacement and velocity. The kinetic temperature, \tilde{T}_n , is calculated by its by its definition (3), where the mathematical expectation is replaced by average over N_R realizations:

$$\tilde{T}_n = \frac{1}{N_R} \sum_{i=1}^{N_R} (\tilde{v}_n|_i)^2, \quad (92)$$

where $\tilde{v}_n|_i$ is the particle velocity for the i -th realization. To obtain the particle velocity, we integrate the Eqs. (91) using the Candy and Rozmus method [92] with the optimization parameters, proposed in [93]. The step of the numerical simulation is performed in accordance with the following scheme, which can be applied due to the weak viscosity¹⁷:

$$\begin{aligned} \tilde{v}_{n,1} &= \tilde{v}_n(\tilde{t}) + a_1 F_n(\tilde{u}_n(\tilde{t}), \tilde{v}_n(\tilde{t})) \Delta\tilde{t} + \tilde{b} \delta_{n,j} \rho_j(\tilde{t}) \sqrt{\Delta\tilde{t}}, & \tilde{u}_{n,1} &= \tilde{u}_n(\tilde{t}) + b_1 \tilde{v}_{n,1} \Delta\tilde{t}, \\ \tilde{v}_{n,2} &= \tilde{v}_{n,1} + a_2 F_n(\tilde{u}_{n,1}, \tilde{v}_{n,1}) \Delta\tilde{t} + \tilde{b} \delta_{n,j} \rho_j(\tilde{t}) \sqrt{\Delta\tilde{t}}, & \tilde{u}_{n,2} &= \tilde{u}_{n,1} + b_2 \tilde{v}_{n,2} \Delta\tilde{t}, \\ \tilde{v}_{n,3} &= \tilde{v}_{n,2} + a_3 F_n(\tilde{u}_{n,2}, \tilde{v}_{n,2}) \Delta\tilde{t} + \tilde{b} \delta_{n,j} \rho_j(\tilde{t}) \sqrt{\Delta\tilde{t}}, & \tilde{u}_{n,3} &= \tilde{u}_{n,2} + b_3 \tilde{v}_{n,3} \Delta\tilde{t}, \\ \tilde{v}_n(\tilde{t} + \Delta\tilde{t}) &= \tilde{v}_{n,3} + a_4 F_n(\tilde{u}_{n,3}, \tilde{v}_{n,3}) \Delta\tilde{t} + \tilde{b} \delta_{n,j} \rho_j(\tilde{t}) \sqrt{\Delta\tilde{t}}, & \tilde{u}_n(\tilde{t} + \Delta\tilde{t}) &= \tilde{u}_{n,3} + b_4 \tilde{v}_n(\tilde{t} + \Delta\tilde{t}) \Delta\tilde{t}, \end{aligned} \quad (93)$$

¹⁶Number of particles is constant in time.

¹⁷For arbitrary viscosity, the modification of the stochastic integrator should be used (see, e.g. [94]).

where $\Delta\tilde{t}$ is time step and

$$\begin{aligned}
a_1 &= 0.51535, & b_1 &= 0.13450, \\
a_2 &= -0.08578, & b_2 &= -0.22482, \\
a_3 &= 0.44158, & b_3 &= 0.75632, \\
a_4 &= 0.12885, & b_4 &= 0.33400.
\end{aligned}
\tag{94}$$

In numerical simulations, the following parameters are used:

$$\Delta\tilde{t} = 0.05, \quad \tilde{b} = 1, \quad N = 512, \quad N_R = 10^5.
\tag{95}$$

For each time step a generated random number ρ_j is uniformly distributed on the segment $[-\sqrt{3}; \sqrt{3}]$, what satisfies the conditions imposed on uncorrelatedness of the random numbers (see Sect. 3).

References

- [1] Dhar, A. Heat transport in low-dimensional systems. *Advances in Physics*, 57(5), 457-537 (2008)
- [2] Anufriev, R., Gluchko, S., Volz, S., Nomura, M. Quasi-ballistic heat conduction due to Lévy phonon flights in silicon nanowires. *ACS nano*, 12(12), 11928-11935 (2018)
- [3] Anufriev, R., Wu, Y., Volz, S., Nomura, M. Quasi-ballistic thermal transport in silicon carbide nanowires. *Applied Physics Letters*, 124(2) (2024)
- [4] Chang, C. W. Experimental probing of non-Fourier thermal conductors. *Thermal Transport in Low Dimensions: From Statistical Physics to Nanoscale Heat Transfer*, 305-338 (2016)
- [5] Vakulov, D., Gireesan, S., et al. Ballistic phonons in ultrathin nanowires. *Nano letters*, 20(4), 2703-2709 (2020)
- [6] Maire, J., Anufriev, R., Nomura, M. Ballistic thermal transport in silicon nanowires. *Scientific Reports*, 7(1), 41794 (2017)
- [7] Cao, A. Molecular dynamics simulation study on heat transport in monolayer graphene sheet with various geometries. *Journal of Applied Physics*, 111(8) (2012)
- [8] Luckyanova, M. N., Garg, J., et al. Coherent phonon heat conduction in superlattices. *Science*, 338(6109), 936-939 (2012)
- [9] Hua, C., Minnich, A. J. Transport regimes in quasiballistic heat conduction. *Physical Review B*, 89(9), 094302 (2014)
- [10] Ding, Z., Chen, K., et al. Observation of second sound in graphite over 200 K. *Nature communications*, 13(1), 285 (2022)
- [11] Cahill, D. G., Ford, W. K., Goodson, K. E., Mahan, G. D., Majumdar, A., et al. Nanoscale thermal transport. *Journal of applied physics*, 93(2), 793-818 (2003)
- [12] Pop, E., Sinha, S., Goodson, K. E. Heat generation and transport in nanometer-scale transistors. *Proceedings of the IEEE*, 94(8), 1587-1601 (2006)

- [13] Li, N., Ren, J., Wang, L., Zhang, G., Hänggi, P., Li, B.: Colloquium: phononics: manipulating heat flow with electronic analogs and beyond. *Rev. Mod. Phys.* 84(1045), 1045–1066 (2012)
- [14] King, S. W., Simka, H., et al. Research Updates: The three M’s (materials, metrology, and modeling) together pave the path to future nanoelectronic technologies. *APL Materials*, 1(4) (2013)
- [15] Ziabari, A., Zebarjadi, M., Vashaee, D., Shakouri, A. Nanoscale solid-state cooling: a review. *Reports on Progress in Physics*, 79(9), 095901 (2016)
- [16] Malik, F.K., Fobelets, K.: A review of thermal rectification in solid-state devices. *J. Semicond.* 43(10), 1–18 (2022)
- [17] Takagishi, M., Narita, N., et al. Microwave assisted magnetic recording: Physics and application to hard disk drives. *Journal of Magnetism and Magnetic Materials*, 563, 169859 (2022)
- [18] Kandeal, A. W., Algazzar, A. M. et al. Nano-enhanced cooling techniques for photovoltaic panels: A systematic review and prospect recommendations. *Solar Energy*, 227, 259-272 (2021)
- [19] Buongiorno, J., Hu, L., et al. Nanofluids for enhanced economics and safety of nuclear reactors: an evaluation of the potential features, issues, and research gaps. *Nuclear Technology*, 162(1), 80-91 (2008)
- [20] Rahnama, Z., Ansarifard, G. R. Nanofluid application for heat transfer, safety, and natural circulation enhancement in the NuScale nuclear reactor as a small modular reactor using computational fluid dynamic (CFD) modeling via neutronic and thermal-hydraulics coupling. *Progress in Nuclear Energy*, 138, 103796 (2021)
- [21] Ren, L., Wang, S., et al. Fouling on the secondary side of nuclear steam generator tube: Experimental and simulated study. *Applied Surface Science*, 590, 153143 (2022)
- [22] Rebay, M., Kakaç, S., Cotta, R. M. (Eds.). *Microscale and Nanoscale Heat Transfer: Analysis, Design, and Application*. CRC Press (2016)
- [23] Rieder, Z., Lebowitz, J. L., Lieb, E. Properties of a harmonic crystal in a stationary nonequilibrium state. *Journal of Mathematical Physics*, 8(5), 1073-1078 (1967)
- [24] A. Casher and J. L. Lebowitz, Heat flow in regular and disordered harmonic chains, *J. Math. Phys.* 12, 1701 (1971)
- [25] Lepri, S., Livi, R., Politi, A. Heat conduction in chains of nonlinear oscillators. *Physical review letters*, 78(10), 1896 (1997)
- [26] V. Kannan, A. Dhar, and J. L. Lebowitz, Nonequilibrium stationary state of a harmonic crystal with alternating masses, *Phys. Rev. E* 85, 041118 (2012)
- [27] Lepri, S., Mejia-Monasterio, C., Politi, A. A stochastic model of anomalous heat transport: analytical solution of the steady state. *Journal of Physics A: Mathematical and Theoretical*, 42(2), 025001 (2008)
- [28] Gendelman, O. V., Paul, J. Kapitza thermal resistance in linear and nonlinear chain models: Isotopic defect. *Physical Review E*, 103(5), 052113 (2021)

- [29] Paul, J., Gendelman, O. V. Kapitza resistance at a domain boundary in linear and non-linear chains. *Physical Review E*, 104(5), 054119 (2021)
- [30] Cane, G., Bhat, J. M., Dhar, A., Bernardin, C. Localization effects due to a random magnetic field on heat transport in a harmonic chain. *Journal of Statistical Mechanics: Theory and Experiment*, 2021(11), 113204 (2021)
- [31] Bhat, J. M., Cane, G., Bernardin, C., Dhar, A. Heat transport in an ordered harmonic chain in presence of a uniform magnetic field. *Journal of Statistical Physics*, 186(1), 2 (2022)
- [32] Gavrilov, S.N., Krivtsov, A.M., Tsvetkov D.V. Heat transfer in a onedimensional harmonic crystal in a viscous environment subjected to an external heat supply. *CMAT*, 31, 255–272 (2018)
- [33] Krivtsov, A. M. Dynamics of matter and energy. *ZAMM-Journal of Applied Mathematics and Mechanics/Zeitschrift für Angewandte Mathematik und Mechanik*, e202100496 (2022)
- [34] Gavrilov, S.N., Krivtsov, A.M.. Steady-state kinetic temperature distribution in a two-dimensional square harmonic scalar lattice lying in a viscous environment and subjected to a point heat source, *CMAT*, 32(1), 41-61 (2019)
- [35] Liazhkov, S. D. Unsteady thermal transport in an instantly heated semi-infinite free end Hooke chain. *Continuum Mechanics and Thermodynamics*, 35(2), 413-430 (2023)
- [36] Gavrilov, S.N. Discrete and continuum fundamental solutions describing heat conduction in a 1D harmonic crystal: Discrete-to-continuum limit and slow-and-fast motions decoupling. *International Journal of Heat and Mass Transfer*, 194, 123019 (2022)
- [37] Gavrilov, S. N., Shishkina, E. V. Non-stationary elastic wave scattering and energy transport in a one-dimensional harmonic chain with an isotopic defect. *Continuum Mechanics and Thermodynamics*, 36(3), 699-724 (2024)
- [38] Kuzkin, V. A., Krivtsov, A. M. (2020). Ballistic resonance and thermalization in the Fermi-Pasta-Ulam-Tsingou chain at finite temperature. *Physical Review E*, 101(4), 042209
- [39] Trunova, I. N., Kuzkin, V. A. Ballistic thermoelasticity of nonlinear chains under thermal shock. *Physical Review E*, 111(1), 014227 (2025)
- [40] Ivanova, E.A. Modeling of thermal and electrical conductivities by means of a viscoelastic Cosserat continuum. *Contin. Mech. Thermodyn.* 34, 555–586 (2022)
- [41] Sokolov, A. A., Krivtsov, A. M., Müller, W. H., Vilchevskaya, E. N. Change of entropy for the one-dimensional ballistic heat equation: Sinusoidal initial perturbation. *Physical Review E*, 99(4), 042107 (2019)
- [42] Shishkina, E. V., Gavrilov, S. N., Mochalova, Y. A. The anti-localization of non-stationary linear waves and its relation to the localization. The simplest illustrative problem. *Journal of Sound and Vibration*, 553, 117673 (2023)
- [43] Shishkina, E. V., Gavrilov, S. N. Unsteady ballistic heat transport in a 1D harmonic crystal due to a source on an isotopic defect. *Continuum Mechanics and Thermodynamics*, 35(2), 431-456 (2023)
- [44] Gavrilov, S. N., Shishkina, E. V., Mochalova, Y. A. An example of the anti-localization of non-stationary quasi-waves in a 1D semi-infinite harmonic chain. In *2023 Days on Diffraction (DD)* (pp. 67-72). IEEE (2023)

- [45] Jackson, E. A. Nonlinearity and irreversibility in lattice dynamics. *The Rocky Mountain Journal of Mathematics*, 8(1/2), 127-196 (1978)
- [46] Hemmer, P.C. Dynamic and stochastic types of motion in the linear chain. *Norges tekniske-hoiskole* (1959)
- [47] Gavrilov, S. N., Krivtsov, A. M. Steady-state ballistic thermal transport associated with transversal motions in a damped graphene lattice subjected to a point heat source. *Continuum Mechanics and Thermodynamics*, 34(1), 297-319 (2021)
- [48] Hoover, W. G., Holian, B. L., Posch, H. A.. Comment I on «Possible experiment to check the reality of a nonequilibrium temperature». *Physical Review E*, 48(4), 3196 (1993)
- [49] Hoover, W. G., Hoover, C. G. Nonequilibrium temperature and thermometry in heat-conducting $\phi 4$ models. *Physical Review E*, 77(4), 041104 (2008)
- [50] Hatano, T., Jou, D.. Measuring nonequilibrium temperature of forced oscillators. *Physical Review E*, 67(2), 026121 (2003)
- [51] Chen, G. Nanoscale energy transport and conversion: a parallel treatment of electrons, molecules, phonons, and photons. Oxford university press (2005)
- [52] Allen, M. P., Tildesley, D. J. Computer simulation of liquids. Oxford university press (1987)
- [53] Gendelman, O. V., Shvartsman, R., Madar, B., Savin, A. V. Nonstationary heat conduction in one-dimensional models with substrate potential. *Physical Review E*, 85(1), 011105 (2012)
- [54] Jepps, O. G., Ayton, G., Evans, D. J. Microscopic expressions for the thermodynamic temperature. *Physical Review E*, 62(4), 4757 (2000)
- [55] Ahmed, H., Nataryan, T., Rao, K.R. Discrete cosine transform. *IEEE Transactions on Computers* C-23(1), 90–93 (1974)
- [56] Hoover, W. G. Computational statistical mechanics. Elsevier (1991)
- [57] Casas-Vázquez, J., Jou, D. Temperature in non-equilibrium states: a review of open problems and current proposals. *Reports on Progress in Physics*, 66(11), 1937 (2003)
- [58] Lepri, S., Livi, R., Politi, A. Thermal conduction in classical low-dimensional lattices. *Physics reports*, 377(1), 1-80 (2003)
- [59] Titulaer, U. M. Ergodic features of harmonic-oscillator systems. III. asymptotic ergodicity. *Physica*, 70(2), 276-296 (1973)
- [60] Puglisi, A., Sarracino, A., Vulpiani, A.: Temperature in and out of equilibrium: a review of concepts, tools and attempts. *Phys. Rep.* 709, 1–60 (2017)
- [61] Zhang, D., Zheng, X., Di Ventra, M. (2019). Local temperatures out of equilibrium. *Physics Reports*, 830, 1-66 (2019)
- [62] Kim, S. Temperature profile and equipartition law in a Langevin harmonic chain. *Journal of the Korean Physical Society*, 71, 264-268 (2017)
- [63] M. A. Guzev, A. V. Gorbunov, Heat flux structure for Ornstein–Uhlenbeck particles of a one-dimensional harmonic chain, *Dal’nevost. Mat. Zh.*, Volume 21, Number 2, 180–193 (2021) (in russian)

- [64] M. A. Guzev, A. A. Dmitriev, Heat flow calculation for a harmonic model of a one-dimensional crystal, *Dal'nevost. Mat. Zh.*, Volume 22, Number 1, 28–37 (2022) (in russian)
- [65] Lykov, A. (2020). Energy growth of infinite harmonic chain under microscopic random influence. arXiv preprint [arXiv:2005.00755](https://arxiv.org/abs/2005.00755).
- [66] Korznikova, E.A., Kuzkin, V.A., Krivtsov, A.M., Xiong, Daxing, Gani, Vakhid A., Kudreyko, A.A., Dmitriev, S.V.: Equilibration of sinusoidal modulation of temperature in linear and nonlinear chains. *Phys. Rev. E* 102, 062148 (2020)
- [67] Sokolov, A. A., Müller, W. H., Porubov, A. V., Gavrilov, S. N. Heat conduction in 1D harmonic crystal: Discrete and continuum approaches. *International Journal of Heat and Mass Transfer*, 176, 121442 (2021)
- [68] Podolskaya, E. A., Krivtsov, A. M., Kuzkin, V. A. Discrete thermomechanics: From thermal echo to ballistic resonance (a review). *Mechanics and Control of Solids and Structures*, 501-533 (2022)
- [69] Kuzkin, V. A., Krivtsov, A. M. Unsteady ballistic heat transport: linking lattice dynamics and kinetic theory. *Acta Mechanica*, 232, 1983-1996 (2021)
- [70] Kuzkin, V. A. Acoustic transparency of the chain-chain interface. *Physical Review E*, 107(6), 065004 (2023)
- [71] Vladimirov, V. *Equations of Mathematical Physics*. Marcel Dekker, New York (1971)
- [72] Krivtsov, A. M. Heat transfer in infinite harmonic one-dimensional crystals. In *Doklady Physics* (Vol. 60, pp. 407-411). Pleiades Publishing (2015)
- [73] Allen, P.B., Nghiem, N.A.: Heat pulse propagation and nonlocal phonon heat transport in one-dimensional harmonic chains. *Phys. Rev. B* 105, 174302 (2022)
- [74] Schrödinger, E.: Zur Dynamik elastisch gekoppelter Punktsysteme. *Ann. Phys.* 349(14), 916–944 (1914)
- [75] Markos, P., Soukoulis, C. M. *Wave propagation: from electrons to photonic crystals and left-handed materials*. Princeton University Press (2008)
- [76] Jankov Maširević, D., Pogány, T. K. Integral representations for products of two Bessel or modified Bessel functions. *Mathematics*, 7(10), 978 (2019)
- [77] Sinko, A. S., Surovtsev, N. V. et al. Polarization Sensitive Raman Scattering and Stimulated Terahertz Emission From GUHP Molecular Crystal. *IEEE Transactions on Terahertz Science and Technology*, 13(5), 526-538 (2023)
- [78] Ryabikin, M. Y. E., Emelin, M. Y. E., Strelkov, V. V. Attosecond electromagnetic pulses: Generation, measurement, and application, attosecond metrology and spectroscopy. *Uspekhi Fizicheskikh Nauk*, 193(4), 382-405 (2023)
- [79] Hoogeboom-Pot, K. M., Hernandez-Charpak, J. N., et al. A new regime of nanoscale thermal transport: Collective diffusion increases dissipation efficiency. *Proceedings of the National Academy of Sciences*, 112(16), 4846-4851 (2015)
- [80] Murachev, A. S., Krivtsov, A. M., Tsvetkov, D. V. Thermal echo in a finite one-dimensional harmonic crystal. *Journal of Physics: Condensed Matter*, 31(9), 095702 (2019)

- [81] Abramowitz , M. and Stegun, I. Handbook of Mathematical Functions: with Formulas, Graphs and Mathematical Tables (Dover, New York, 1972)
- [82] Temme, N.M. Asymptotic Methods for Integrals (2014).
- [83] Vasiliev, V. V., Lurie, S. A. Differential equations and the problem of singularity of solutions in applied mechanics and mathematics. Journal of Applied Mechanics and Technical Physics, 64(1), 98-109 (2023)
- [84] Northrop, G. A., Wolfe, J. P. Phonon imaging: Theory and applications. In Nonequilibrium Phonon Dynamics (pp. 165-242). Boston, MA: Springer US (1985)
- [85] Northrop, G. A., Wolfe, J. P. Ballistic phonon imaging in germanium. Physical Review B, 22(12), 6196 (1980)
- [86] Koos, G. L., Wolfe, J. P. Phonon focusing in piezoelectric crystals: Quartz and lithium niobate. Physical Review B, 30(6), 3470 (1984)
- [87] Stepanov, S.: Stochastic World. Springer, Berlin (2013)
- [88] Kunin, I. A. Elastic media with microstructure I: one-dimensional models (Vol. 26). Springer-Verlag (1982)
- [89] Charlotte, M., Truskinovsky, L. Lattice dynamics from a continuum viewpoint. Journal of the Mechanics and Physics of Solids, 60(8), 1508-1544 (2012)
- [90] Liazhkov, S. D. Energy supply into a semi-infinite β -Fermi–Pasta–Ulam–Tsingou chain by periodic force loading. Acta Mechanica, 1-23 (2024)
- [91] Hall, Brian C. Lie Groups, Lie Algebras, and Representations. Springer (2015)
- [92] Candy, J., Rozmus, W.: A symplectic integration algorithm for separable Hamiltonian functions. J. Comput. Phys. 92(1), 230–256 (1991)
- [93] McLachlan, R.I., Atela, P.: The accuracy of symplectic integrators. Nonlinearity 5(2), 541–562 (1992)
- [94] Skeel, R. D., Izaguirre, J. A. An impulse integrator for Langevin dynamics. Molecular Physics, 100(24), 3885-3891 (2002)